ABSTRACT

Title of Document:	**ABORT TRAJECTORIES FOR MANNED LUNAR MISSIONS**
	E. David Beksinski Jr. Master of Science, 2007
Directed By:	Professor Mark J. Lewis Department of Aerospace Engineering

With NASA's renewed focus towards a permanent human presence on the moon, comes the development of the Crew Exploration Vehicle. Unforeseen circumstances can induce emergency situations necessitating contingency plans to ensure crew safety. It is therefore desirable to define the feasibility of a direct abort from an outbound translunar trajectory. Thus an astrodynamic model for lunar transfer has been developed to allow for characterization of the abort feasibility envelope for conceivable transfer orbits. In addition the model allows for several trade studies involving differently executed abort options, factoring in fuel margins. Two optimization schemes were utilized; one to expedite return via any fuel in excess of that required for the abort, and one to explore the boundary region of direct abort infeasibility envelope searching for plausible abort trajectories.

The characterization and optimization of translunar abort trajectories for the Crew Exploration Vehicle can ensure increased crew survivability in emergency situations.

ABORT TRAJECTORIES FOR MANNED LUNAR MISSIONS

By

E. David Beksinski Jr.

Thesis submitted to the Faculty of the Graduate School of the
University of Maryland, College Park, in partial fulfillment
of the requirements for the degree of
Master of Science
2007

Advisory Committee:
Professor Mark J. Lewis, Chair
Professor Darryll J. Pines
Professor Roberto Celi

Dedication

To my parents and family whose love and support has given me so much more then I ever thought possible. Thank you for everything Mom and Dad.

Acknowledgements

Table of Contents

List of Tables

List of Figures

Nomenclature

$\boldsymbol{e}$ Specific Mechanical Energy [km^2/s^2]

$\boldsymbol{f}$ Flight Path Angle [deg]

$\boldsymbol{m}$ Gravitational Constant [km^3/s^2]

$\boldsymbol{n}$ True Anomaly

a   Semi-Major Axis [km]

a_x Acceleration X-direction [km/s^s]

a^y Acceleration Y-direction [km/s^s]

c   Foci Displacement [km]

e   Eccentricity

h   Angular Momentum [km^2/s]

p   Semi-Latus Rectum [km]

r   Radius (Magnitude of radius vector) [km]

r_a Apoapsis Radius [km]

r_p Periapsis Radius [km]

E   Eccentric Anomaly

M   Mass [kg]

T   Time of Flight [s]

V   Velocity [km/s]

ΔV Delta Velocity [km/s]

V_x Velocity X-direction [km/s]

V_y Velocity Y-direction [km/s]

X   X Position [km]

Y   Y Position [km]

Acronyms

AS   Ascent Stage

CEV   Crew Exploration Vehicle

CM   Command Module

CSM   Command/Service Modules (docked configuration)

DS   Descent Stage

EDS   Earth Departure Stage

FRT   Free Return Trajectory

GNC   Guidance, Navigation, & Control

LEO   Low Earth Orbit

LLO   Low Lunar Orbit

LOI   Lunar Orbit Insertion

LSAM   Lunar Surface Access Module

LA   Lunar Ascent

LD   Lunar Descent

LV   Launch Vehicle

RFP   Request For Proposal

RCS   Reaction Control System

SM   Service Module

TDRS   Tracking and Data Relay Satellite

TEI   Trans-Earth Injection

TLI   Trans-Lunar Injection

Chapter 1.   Introduction

This chapter explains the motivation for this study as well as outlines the general format and goals of the study. A review of past abort trajectory work for the Apollo program is included in the final section.

1.1.   Motivation

The current goal set forth by NASA is to conduct a manned lunar mission in 2018.[1] Initial plans are superficially similar to the Apollo program, though with exceptions of larger crew and increased lunar surface mission duration. Safety will certainly be an issue for any lunar mission, and while significant measures are taken to mitigate risk to the crew, sending people 378,000 km above the surface of the Earth and landing them on the Moon carries an inherent risk. Although mission planning will be performed to excruciating detail, the fact remains that it can only account for any foreseeable circumstance. Even with system redundancy and designing for zero single point modes of failure, problems may arise requiring rapid return to Earth. The Apollo spacecraft had limited transit abort capability; it is a reasonable goal that any future lunar transit mission should be able to be performed with greater efficiency, and most importantly, a greater margin of safety.

The need for contingency plans in case of an emergency in transit to the moon is most blatantly illustrated by the case of the Apollo XIII mission. Mechanical failure of a fan in one of the oxygen tanks sparked and caused a massive system failure and subsequent explosion. This induced an emergency situation which was mitigated by conservation of available power and life support resources and also via use of the Free Return Trajectory (FRT). Every Apollo mission, as well as presumably any future missions, have or will utilize a FRT or hybrid trajectory limited by FRT abort constraints. A FRT lunar transfer is characterized by its zero delta velocity (ΔV) requirements for return to Earth. Once the Trans-Lunar Injection (TLI) burn is initiated in Low Earth Orbit (LEO), if no other control burns are conducted, the spacecraft will slingshot around the Moon and return to proper re-entry interface. This subset of lunar trajectories is utilized such that in the event of an engine failure or other type of emergency, the spacecraft will still return to Earth. Whereas, with a non-FRT, without a decelerating burn in proximity to the moon, the spacecraft could fly past the moon and move beyond a point of possible return. Hence the motivation for utilization of a FRT for any manned mission is readily apparent.

The exception to this rule is hybrid trajectories, where the FRT is departed from during the initial translunar trajectory by a midcourse correction, in order to gain a fuel advantage allowing more expansive lunar access. While the hybrid trajectories can allow a fuel savings, it is not done so at the cost of safety. The

hybrid trajectories are bounded by the abort capabilities of the spacecraft, such that if a main engine failure occurred, an abort procedure could be performed which would place the spacecraft on a direct return to a re-entry trajectory. The application of these hybrid trajectories would therefore be highly dependant on a well defined design space of abort trajectory options and spacecraft capabilities.

Motivation for a study of abort feasibility and optimized return is readily apparent in the Crew Exploration Vehicle (CEV) Technical Requirements, as explained in the Request For Proposal (RFP) released by NASA. The following three requirements directly quoted from the RFP Section 6.0 CEV Technical Requirements[2] pertain directly to the need for this research:

Req. #2.   Provide an abort capability during all phases of flight.

Req. #10.   Be capable of return from lunar orbit to the earth surface without assistance from external Constellation elements.

Req. #12.   Abort capability independent of Launch Vehicle (LV) or Earth Departure Stage (EDS) flight control.

With reference to requirement number two, abort capability could imply use of FRT or direct abort; as it will be shown that ΔV cost requirements for certain mission phases are prohibitively high. Requirement number ten seems to imply that the CEV must have a ΔV budget sufficient to return to Earth without refueling or any other required support from lunar based assets. Lastly requirement number twelve indicates the CEV must have an abort capability

independent of LV and EDS stages. The EDS stage is the stage that provides the TLI burn initiating the lunar transfer orbit. As will be discussed, this sets the basis for the CEV ΔV budget based on the assumption that the LV and EDS will not be required or available for utilization by the CEV for the remainder of the lunar mission. In addition, upon completion of the TLI burn, the large ΔV maneuver has already been imparted upon the spacecraft to attain lunar orbit altitude. The spacecraft subsequent to the TLI maneuver will have high velocity and the EDS propulsion system will be depleted, thus negating any possible gain from its use during an abort. Figure 1.1 shows the representative Apollo mission profile, which was used as a baseline for this analysis of future missions.
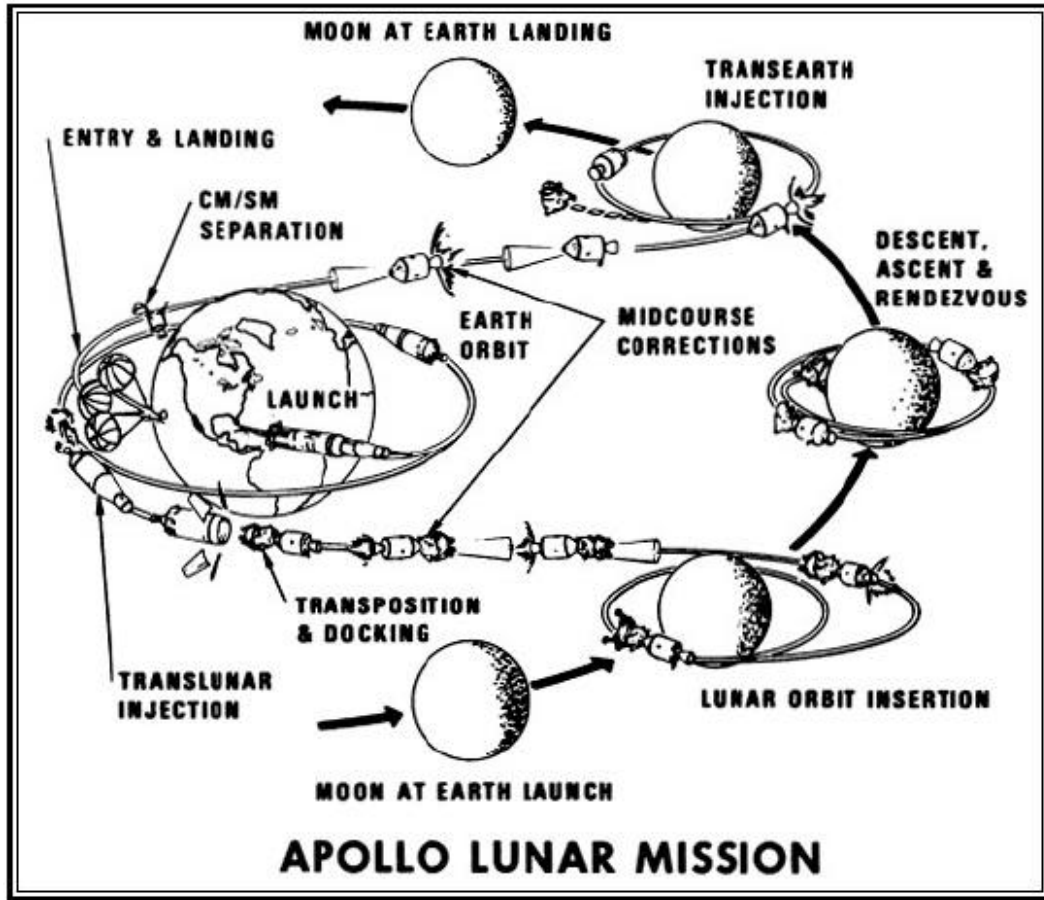
Figure 1.1 Representative lunar mission profile

While the possibility for an emergency situation arising from any single mechanical, environmental or health concerns is slight; failures of these types occur routinely on manned spacecraft. Although contingencies for these concerns can be planned for, it is namely the concerns which have not been thought of that preclude the necessity for sound and reliable mission abort scenarios.

1.2. Research Objectives

The primary research objective is naturally to specifically characterize the feasibility of a direct abort at any time during lunar transit. The characterization will form a direct abort feasibility profile from which abort feasibility can be determined quickly by inspection across the duration of the translunar trajectory.

A secondary research objective is based upon the abort feasibility profile. It is reasonable to presume that as the ΔV requirement for direct abort varies, during segments of the translunar trajectory when a direct abort is feasible, the amount of ΔV available can exceed the direct abort requirement. Therefore the goal of optimal usage of any excess fuel to attain a higher energy return trajectory would be beneficial to crew survivability via reduction of time of flight to re-entry.

Once the direct abort feasibility has been characterized and higher energy trajectory options have been explored, a final research objective is to survey the trajectory design space for other possible options. A similar optimization scheme to the secondary research objective is used to explore the boundary of the infeasibility region. An effort to find any possible return trajectories utilizing multiple trajectory segments could offer further options for the crew in an abort scenario.

1.3.   Thesis Overview

Chapter 1 covers and introduction to the problem and a review of previous abort studies conducted for the Apollo missions. A detailed rationale for direct aborts as well as spacecraft overview is given in Chapter 2. Also included in Chapter 2 is the development of four different abort staging strategies and their impact on available ΔV for the spacecraft. Chapter 3 outlines the development of the astrodynamic model utilized for the abort feasibility study. Chapter 4 explains the two different optimizations utilized; one to achieve a faster return time via utilization of any fuel left after a direct abort, and a second to search the abort trajectory design space for trajectories consisting of multiple course corrections. A typical translunar trajectory is thoroughly analyzed and explained in Chapter 5. Lastly, Chapter 6 outlines the impacts of this study on future manned lunar missions.

1.4.   Previous Lunar Abort Work

Unmanned lunar bound spacecraft such as the Lunar Prospector mission launched in January of 1998 can offer some insight along similar trajectories to those used for Apollo and soon the CEV. The Lunar Prospector utilized a trajectory characterized by a 105 hour time of flight; a lesser degree of orbital transfer energy than the approximately 72 hour transit times for Apollo.[3]

Important facts that can be taken from this mission for abort scenarios include the use of NASA Tracking and Data Relay Satellite (TDRS) for accurate real time telemetry information. Accurate telemetry data combined with three trajectory correction maneuvers allowed mission controllers to place the spacecraft within 10 miles of its targeted lunar orbit altitude and within .1 degrees of the target inclination. Use of telemetry data from the TDRS confirmed engine burn ΔV maneuvers were within 1% of targeted values.[3] The conglomeration of this information has a positive impact on the outlook for future lunar mission abort scenarios. Given the accurate telemetry data available, as well as engine performance metrics, it can be established with confidence that the exact location and ΔV capabilities of the CEV can be ascertained throughout the mission. Vitally important for any abort trajectory maneuver is an accurate knowledge of starting position and velocity, which is crucial to ensuring safe transit into the re-entry corridor.

Previous studies of abort feasibility and trajectories are primarily centered on the Apollo program as this is the only other program involving manned lunar missions. As with the CEV RFP requirements, an operational constraint of the Apollo missions stipulated that the spacecraft must be able to return the crew safely to Earth from any point during the mission.[4] Spacecraft return can be accomplished via a combination of available abort trajectories and also utilization of a free return trajectory. It was known that in a certain range along

the translunar trajectory the ΔV requirements were prohibitively high. Thus any abort would either have to rely on the FRT to come back to Earth or wait until a direct abort becomes feasible.

Two major classes of aborts were examined previously for Apollo; minimum ΔV abort trajectories and minimum time of flight abort trajectories. Minimum ΔV abort trajectories define the lowest possible ΔV requirements for return to Earth, unbounded by constraints of landing at a predetermined location. Landing site constraints were removed due to the added ΔV requirement of any such landing site constraints. Minimum time of flight abort trajectories are directly dependant on both available propulsion capabilities and position along the translunar trajectory.[5]

In an effort to increase the lunar landing site range for the Apollo program hybrid trajectories were studied and utilized on the Apollo 14 mission.[6] The hybrid trajectory allows a larger possible design space of translunar trajectories by relaxation of the free return trajectory constraint. Hybrid trajectories could be engaged in two ways. The first involves the injection of the spacecraft into a TLI trajectory that satisfies the free return trajectory constraint, followed five to ten hours later subsequent to a comprehensive propulsion and guidance systems check, by a mid-course correction maneuver placing the spacecraft on a non-free return trajectory. The second method involves a direct injection at TLI into a non-free return trajectory. In relaxing the free return

trajectory constraint, a surrogate constraint was imposed on the mission design criteria. All hybrid trajectories must satisfy an abort constraint based on the lunar module descent propulsion system in the event that the service module propulsion system failed at lunar orbit insertion.[6]

Optimization schemes were also previously developed by Bass in 1970 to minimize the total ΔV for the Apollo hybrid trajectory missions. The energy level of the hybrid trajectory was bounded on the lower range by the descent propulsion system abort capabilities, and on the high end by the ΔV cost of a similar mission along a free return trajectory. Optimization schemes enabled hybrid trajectories that could reach areas of the lunar surface previously out of the feasible mission required ΔV range for the Apollo spacecraft. An important special case arose out of the optimization; that for landing sites far from the lunar equator, the abort ΔV requirement always exceeded the abort capabilities.[7]

The high ΔV requirement for an abort from trajectories to lunar polar regions could influence the design of the CEV, as one of the design criteria stipulates global lunar access. While the utilization of hybrid trajectories can facilitate this goal; propulsion capabilities of the lunar module should be designed to provide adequate abort capacity for global lunar access. Figure 1.2 illustrates the hybrid trajectory concept.

HIGH PERISELENE
FREE RETURN TRAJECTORY

MOON

(a)
FREE RETURN

EARTH

TLI

UNABORTED TRAJECTORY

MOON

ABORT
POINT

(b)
ABORT FROM NON FREE RETURN

EARTH

TLI

HYBRID
POINT

LOI

MOON

TEI

LUNAR
ORBIT

(c)
NOMINAL HYBRID TRAJECTORY

EARTH

TLI
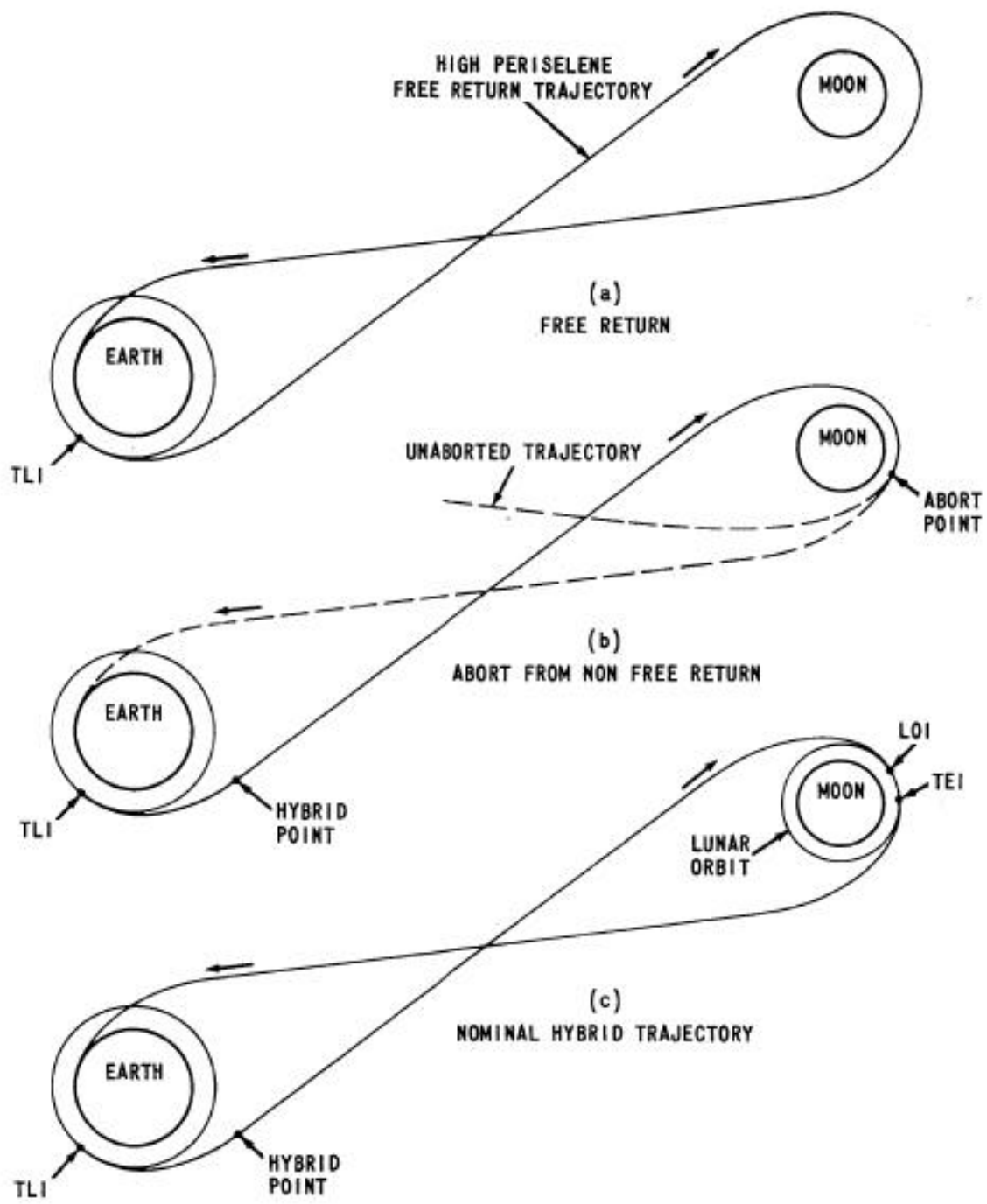
HYBRID
POINT

Figure 1.2 Hybrid translunar trajectories [7]

Another significant concept studied for the Apollo program involves increasing abort capabilities of the spacecraft via jettisoning the service module. Utilization of the lunar module descent propulsion system for abort burns could be possible in the event of service propulsion system failure at lunar orbit insertion. Primary reasoning for this strategy lies in reducing the spacecraft's mass such that the lunar module descent propulsion system has an increased effective ΔV capability. The lunar module ascent system was not considered for utilization due to insufficient Reaction Control System (RCS) capabilities to control the spacecraft with the command and service module still docked.[8] From this fact an important design criterion for the CEV lunar module can be drawn. In order to allow for maximum flexibility in off-design spacecraft configurations, primarily extreme abort situations, the RCS system for each module should be robust enough to control the spacecraft when at its maximum possible mass.

The "Translunar Abort Techniques for Non-Free-Return Missions"[8] study for Apollo centered on the assumption of service module propulsion failure at lunar orbit insertion, implying that fuel tanks would be virtually full. With no way to transfer fuel between the service module and lunar descent modules, the service module fuel allotment becomes unutilized, dead mass. It is with this in mind that it was recommended to jettison the service module. The reduction in mass of the total spacecraft increased the effective ΔV of the lunar module descent stage roughly 70% from 2700 feet per second to 4600. The increase in ΔV

made a single burn abort trajectory of approximately 3400 feet per second a feasible option.[8]

Jettisoning the service module requires the lunar module to provide life support for the crew during the return trajectory as the command module would be required to shut down to conserve resources. Creating a dependency of three crew members on a life support system designed for a crew of two implies an added time constraint in return trajectories. Upon reaching the re-entry interface the crew would enter the command module and jettison the lunar module for re-entry. The principle strategy of reduction of spacecraft mass to improve effective ΔV of available propulsion systems will become central to several different abort methods.

A final abort concept studied in the Apollo program is that of a manual abort. In an emergency situation it is necessary to consider the ramifications of partial or total loss of guidance and navigation. With this in mind a procedure was developed involving a visually guided abort maneuver utilizing the docking reticle to target Earth. In this situation the target landing site constraint has been removed, due to emergency conditions, a fastest time to return is preferable over landing site specification. It was found that there exists a preferred abort station along a given translunar trajectory for manual abort. This station is defined by a maximum allowable error tolerance on ΔV while maintaining safe re-entry corridor conditions. For the standard Apollo reference trajectory this point

occurs approximately 31 hours after the initial translunar injection burn. At this point an allowable ΔV dispersion of plus or minus 450 feet per second exists.[9] The manual abort targeting method was partially flight verified during the Apollo XIII mission. Although Apollo 13 utilized the free return trajectory abort option, a midcourse correction was performed using the Earth viewed through the docking reticle method during the return leg of the mission. While complicated and very difficult to perform it was proven feasible.

Due to similarities in spacecraft architecture between the Apollo and CEV design much of the previous work can be applied to the new. While differences in the CEV design can lead to differing abort strategies, the fundamental motivations and concepts of Apollo abort studies lay a comprehensive foundation for any future lunar mission abort strategy.

Chapter 2. Abort Methodology

The motivation for a comprehensive abort trajectory study has been given in Chapter 1, this chapter starts with an explanation of what causes could necessitate a direct abort. Next follows an overview of a typical mission, as well as identifying spacecraft masses and propulsive capabilities. From these masses and ΔV capabilities, four different abort staging methods can now be developed.

2.1. Abort Rationale

2.1.1.   Mechanical Failures

As with any other mechanical system, the CEV will almost certainly encounter occasional failures. Any system is only as reliable as its least reliable component.   The complexity of the spacecraft and the environments it is designed to operate in compound the strain on the spacecraft. Even prior to launch the spacecraft is subjected to various physical loads during assembly and launch preparation.

The cause of the Apollo XIII incident has been traced back to launch preparations where the affected oxygen tank was allowed to slip and fall only a few inches during installation. This single event caused some heater wires inside

the tank to loosen just enough to be exposed to oxygen, eventually leading to the catastrophic failure of the tank and the resulting mission crisis.

Acceleration forces can impart strong loading conditions on the spacecraft as it is propelled into orbit. Once in orbit, various environmental concerns such as: radiation, thermal loading, space debris, and internal spacecraft pressurization against vacuum, can all impart physical loads on the systems.

Material defects can also cause concern. Small imperfection in materials undetectable to the eye can cause failure of mechanical components long before their designed failure limit.

All of the above listed mechanical concerns are planned for and every step is taken to avoid such failures via quality assurance practices and redundant design characteristics. However it is not possible to attain total assurance against all these issues and therefore abort scenarios for mechanical failures are situations that must be planned for.

2.1.2. Environmental Conditions

The Earth offers protection from many environmental hazards; the spacecraft can protect the crew to a certain degree, but cannot be a guaranteed haven. Radiation is of key concern. While the spacecraft can offer shielding, the sheer mass of shielding required to block all radiation is prohibitively high. The boundary of the magnetosphere is approximately 95000 km above the surface of

the Earth.[10] Implying that during any given manned lunar mission, the crew can rely on the Earth's magnetosphere for protection from solar events only for less than the first 25% of the journey.

Compounding the radiation concern is the insufficient understanding and prediction of solar events. The eleven year cycle of maximum solar activity is somewhat understood, however only on a statistical basis. Virtually all predictive solar activity models to date are based on a statistical analysis of observation records.[10] While these statistical models can form a reasonable basis of understanding for mission planning, they are not founded on a physical understanding of solar activity. The implication is that predicting a solar event based on physical evidence or precursors to a solar flare is not possible, and therefore warning time is on the order of hours. However statistically unlikely a major solar eruption is during any given mission, the fact remains it is something that cannot be determined far enough in advance to postpone launch. Therefore a fastest return to Earth abort is an entirely necessary situation to avoid potentially fatal radiation exposure.

NASA's long term goals also have an effect on the need for abort trajectories due to solar events. President George W. Bush[11] and NASA Director Michael Griffin have both stressed the importance of a permanent human presence in space and the importance of a permanently manned lunar base both for operations in both Earth-Lunar space as well as interplanetary space to Mars

and beyond. A major implication of this level of space operations is a drastic increase in manned space flight frequency over the next few decades. While missions can be planned around statistical predictions of solar activity, and any likely lunar base would have a radiation shielded "fallout" type shelter for solar storms; any spacecraft in transit during a solar event will likely need to at minimum abort to LEO for shelter.   Frequent re-supply and crew transfer missions increase the odds of an in-transit solar event necessitating a direct abort.

Another space environmental hazard is space debris and micro meteorites. Significant effort is placed in tracking space debris and Earth-crossing asteroids. However there is a limit on how many objects can be tracked.[12] The closing speeds of any object on a collision course with a spacecraft makes even a fleck of paint dangerous. Impacts on the spacecraft from such debris do occur and could potentially cause enough damage to necessitate an abort scenario.

2.1.3.   Unanticipated Hazards

The subject of unanticipated hazards is a final category that covers anything else that could go wrong. A large concern is emergency healthcare in space. Although astronauts endure a rigorous selection criteria, and strict health examinations, the possibility for some unforeseen medical condition will always be present. Medical training is mandatory for at least one member of the flight

crew, but limited training cannot come close to meeting the needs as a professional doctor could. Medical equipment has advanced to assist in emergency requirements such as portable defibrillators and pre-dosed auto injection syringes allowing for a fairly substantial medical coverage in a relatively small package for the spacecraft. However, in the event of an astronaut requiring professional medical care, the spacecraft should perform the function of an ambulance; stabilize and transport the patient to a medical facility. In light of limited resources combined with difficulties in providing care due to micro gravity effects, it is unreasonable to expect any transport spacecraft to offer the medical equivalent of a trauma center. Such capabilities may one day be realized on a larger space station, however for the present CEV and similar vehicles, emergency medical care would prompt a direct abort scenario. Although contingencies for any anticipated concerns can be planned for, it is namely the concerns which have not been thought of that necessitate the need for mission abort scenarios.

2.2. Mission Overview

A typical manned lunar mission consists of five major engine firing events. Each propulsive maneuver initiates a primary phase of the mission.

First the Trans-Lunar Injection (TLI) maneuver is conducted. The propulsion system responsible for this engine burn is the Earth Departure Stage

(EDS). Generally, as was the case for the Apollo spacecraft, the EDS is the top stage of the launch vehicle, thus the ΔV requirement for TLI does not bear on the spacecraft design. Once the TLI burn is completed the spacecraft coasts until the lunar interface has been reached.

At this point the spacecraft must complete the Lunar Orbit Insertion (LOI) maneuver. The LOI propulsive burn injects the spacecraft into a circum-lunar orbit. The circum-lunar orbit, also known as Low Lunar Orbit (LLO) is typically on the order of 100 km above the lunar surface and serves as the parking orbit for the service and command modules of the spacecraft during lunar surface excursions in the lander modules.

Once the spacecraft has achieved LLO, the next phase of the mission is conducted by the lunar lander. The Lunar Descent (LD) mission phase is the propulsive burden of the lunar descent module. As will be important later in mass ratio calculations, it is important to note that the service and command modules remain in LLO, and only the lunar module descent and ascent stages descend to the lunar surface.

Following surface excursion activities the next phase of the mission is that of Lunar Ascent (LA). The LA maneuver is performed by only the lunar module ascent stage, as the descent stage is left on the surface. The crew then docks with the command and service modules for the return trip to Earth.

The last mission phase is initiated by the Trans-Earth Injection (TEI) maneuver. This engine burn imparts the spacecraft onto a coasting trajectory directly into the re-entry interface upon return to Earth.

2.3. Baseline Case: Apollo Mass/Propulsion Data

When developing a set of abort strategies to study, it is necessary to establish a baseline case from which to build various abort options. The Apollo missions are the only previous example of manned lunar missions and thus an obvious choice. At the time of development, final mass estimations for the CEV were not yet available, thus the masses and propulsion capabilities of the Apollo spacecraft modules formed a reasonable basis for model development. Table 2.1[13,14,15] shows statistics on individual modules utilized during the initial study. It is important to note that the ΔV capabilities listed are only for the specified module. As will be discussed later, a propulsion system's effective ΔV when docked with other modules is calculated via mass ratios of the docked modules.

Table 2.1 Apollo spacecraft mass and propulsion data

Module	Mass (kg)	Delta V (km/s)
Command	5,806	N/A RCS Only
Service	24,523	2.804
Lunar Descent	10,149	1.762
Lunar Ascent	4,547	1.730

2.4. CEV Mass/Propulsion Data

In December of 2005, NASA released a report entitled "NASA's Exploration Systems Architecture Study (ESAS)."[1] The ESAS report detailed the recommendations for the new CEV architecture. Every conceivable system architecture was evaluated and a final architecture was presented. It was decided that the CEV would retain the basic module structure of Apollo, however with some key changes. The modules would be sized for a crew of six and designed for extended lunar surface mission durations of the entire crew. The command and service module is to be left unmanned in low lunar orbit during surface excursions. As shown in Table 2.2[1], this results in a comparatively larger lunar module than that of Apollo. Other notable changes include increased ΔV capability of the lunar module to afford global lunar access. In a departure from the Apollo architecture, the service module propulsion system is only responsible for the Trans-Earth Injection (TEI), while the Lunar Surface Access Module (LSAM) descent stage assumes responsibility for the

Lunar Orbit Insertion (LOI) maneuver. Again as with the Apollo data, the ΔV listed in Table 2.2, is the capability of each CEV module alone, different staging options offering various effective ΔV's for varying abort strategies will be addressed via mass ratios.

Table 2.2 CEV spacecraft mass and propulsion data

Module	Mass (kg)	Delta V (km/s)
Command	9,506	N/A RCS Only
Service	13,647	1.450
Lunar Descent	35,055	3.290
Lunar Ascent	10,809	1.866

2.5. Abort Staging Methods

Four separate abort staging methods were investigated for this study. Since both the Apollo and CEV spacecraft have similar basic module architecture all four methods are applicable to either spacecraft. Differences in relative module mass fractions affect the effective ΔV for each method. The effective ΔV available in each method is directly related to the abort capability during the translunar trajectory. The feasibility of performing an abort maneuver increases with increasing effective ΔV. Figure 2.1 illustrates the symbols used throughout the descriptions of the four abort methods.

Module/Key	Symbol
Command	
Service	
Lunar Descent	
Lunar Ascent	
Indicates Engine Firing	
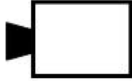
Figure 2.1 Abort methods legend

2.5.1.   Nominal Abort

The nominal abort staging option provides a direct abort capability while maintaining a standard mission spacecraft module configuration.   In this method, the lunar module propulsion system is utilized, first descent stage following by descent stage jettison and burn of ascent stage engine. Next the service module propulsion system is utilized. For the duration of the return flight time the service module, command module and lunar ascent module remain docked affording the maximum possible living space and, conceivably, consumable resources. The service module and lunar ascent module would be jettisoned just prior to re-entry as in a typical mission.   This method is

24

summarized in Table 2.3. For clarity the current staged burn has been indicated

by a small flame symbol.

Table 2.3 Nominal abort method

	1st Engine Burn	2nd Engine Burn	3rd Engine Burn
Nominal Abort			
Apollo Effective Delta V (km/s)			3.084
CEV Effective Delta V (km/s)			4.235
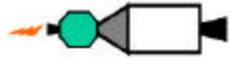
The nominal abort configuration offers the maximum possible allotment

of resources during the abort trajectory. By retaining the lunar module ascent

stage until just prior to re-entry the habitable volume is dramatically increased.

For the Apollo spacecraft, the habitable volume of the command module is 6.17

cubic meters, while the lunar module ascent stage is 6.65 cubic meters.[14,15] The

addition of the lunar ascent module more then doubles the habitable volume for

the crew during the duration of the abort trajectory. While the CEV will be

designed for a larger crew it is likely that the habitable volumetric ratio between

the CEV command module and the lunar ascent module will remain in the

approximate range of the Apollo spacecraft modular volumetric ratio. In

addition, with the design criterion of extended lunar surface excursions, it is

likely the CEV lunar module will retain a significant habitable volume. Tandem

to the habitable volume increase will be an inherent life support capability

comprised of the combined resources from the command module and lunar ascent modules.

2.5.2.   Ideal Abort

The ideal abort method summarized in Table 2.4 below is very similar to the nominal abort. The difference is that prior to the final engine burn by the service module the lunar ascent module is jettisoned. The lunar module jettison is performed as a sacrifice of habitable volume and potentially usable consumable supplies still in the lunar module in exchange for decreasing the mass. For the Apollo spacecraft this mass advantage affords an extra kilometer per second of effective ΔV. The effective ΔV gain for the CEV is still significant, approximately half a kilometer per second of ΔV, however not as large as the gains the Apollo spacecraft achieved due to the reduced size of the service module. The service module for the CEV only performs the TEI burn, whereas the service module for Apollo performed the LOI and TEI burns, thus the CEV service module has comparatively less ΔV to start with, reducing the gain in effective ΔV.

Table 2.4 Ideal abort method

	1st Engine Burn	2nd Engine Burn	3rd Engine Burn
Ideal Abort			
Apollo Effective Delta V (km/s)			4.094
CEV Effective Delta V (km/s)			4.697
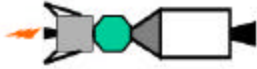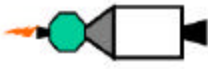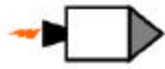
Although the ideal abort method involves the jettisoning of the lunar ascent module and thereby sacrifice of any available resources contained therein; the CEV design will likely assist in mitigating any negative effects. Based on the CEV design criterion of the service module remaining un-manned in low lunar orbit for durations on the order of weeks to months, the service module is designed with solar panel power supply.[1] During the course of the Apollo XIII mission abort, it was necessary to retain the lunar module for life support as well as for power to re-start the command module guidance navigation and control computer prior to re-entry. With the addition of solar panels, a non consumable power supply is available to charge spacecraft batteries; contrary to the oxygen consuming fuel cells of the Apollo spacecraft. It can reasonably be presumed that a small amount of consumables, such as water and food could be transferred to the command module prior to jettisoning the lunar module. This combined with the solar power capability could help mitigate the negative drawbacks to jettisoning the lunar module.

2.5.3.   Lifeboat Case 1 Abort

The lifeboat case 1 abort method is the first of two methods devised to afford the largest mass fraction advantage via module staging, as overviewed in Table 2.5. The concept relies on utilization of the lunar module ascent stage as a lifeboat of sorts. For the Apollo spacecraft the largest modules by mass are the lunar module descent stage and the service module. By utilizing the available fuel in the service module first, jettisoning it, and subsequently burning the available fuel in the lunar module descent stage and jettisoning it as well, the last burn by the lunar module ascent stage achieves the lightest mass ratio possible. The Apollo spacecraft affords approximately 300 additional meters per second of ΔV in this manner. Of note for the CEV is that effective ΔV is actually less then that of the ideal abort case. The lifeboat case methods were derived prior to the release of the ESAS report and the subsequent mass specifications for the CEV modules rendered the two lifeboat methods less then optimal due to the sizing and differing propulsion responsibilities of the modules.

Table 2.5 Lifeboat case 1 abort method

	1st Engine Burn	2nd Engine Burn	3rd Engine Burn
Lifeboat 1 Abort			
Apollo Effective Delta V (km/s)			4.306
CEV Effective Delta V (km/s)			4.443
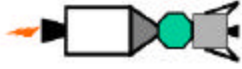
While the loss of the service module resources imposes a serious limitation on the life support capabilities of the spacecraft, it is potentially a sacrifice made to gain a time advantage to return of the crew. The combined available power of the command module with that of the lunar ascent stage would be of key concern, as well as, the oxygen available for life support. This extremely life support limited method would likely be utilized in situations where the return time was on the order of 10 to 15 hours; with such short return time of flight the primary consumable resource concern is reduced to oxygen for breathing. Presumably, the gain in return time outweighs the need for water for the crew during the return. The lifeboat method therefore has potential merit for abort trajectories initiated early in the outbound translunar trajectory, though bounded in practicality by the power and life support capabilities of the spacecraft lunar ascent and command modules.

2.5.4.   Lifeboat Case 2 Abort

The lifeboat case 2 abort method, illustrated in Table 2.6, is very similar to its previous counterpart. This method simply switches the order of the first 2 stages, the lunar module descent stage and the service module. It was predicted that this would not improve the effective ΔV for the Apollo spacecraft. However due to ease of integration via mass ratios it was deemed worthy of examination. Unfortunately, upon inclusion of the updated CEV mass and propulsion capabilities it proved even less beneficial. The methods retention, if nothing else, serves to illustrate via comparison the benefits of the other three abort methods, reinforcing the merits of their utilization.

Table 2.6 Lifeboat case 2 abort method

	1st Engine Burn	2nd Engine Burn	3rd Engine Burn
Lifeboat 2 Abort			
Apollo Effective Delta V (km/s)			4.223
CEV Effective Delta V (km/s)			4.132
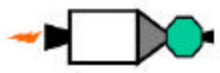
Although mass ratios involved with this abort method preclude the practicality of its utilization, the same life support constraints as the first lifeboat abort method apply equally to this method.

Chapter 3.   Astrodynamic Model Development

Now that spacecraft propulsive capabilities and various abort methods have been discussed in Chapter 2; this chapter outlines the creation of an astrodynamic model.   It flows from the characterization of a translunar trajectory, to the method of determining direct abort ΔV requirements.

3.1.   Algorithm Overview

The lunar transit is the mission phase of most concern and uncertainty during emergency situations. This is defined as the period of time after TLI burn, but before Lunar Orbit Insertion (LOI) burn, as was shown in Figure 1.2. Aborts performed during lunar transit are the most critical for several reasons, in mission phase order:

1)   <u>Prior to the TLI burn in LEO</u> an abort and subsequent re-entry will be relatively straightforward, as the TLI energy has not yet been imparted on the spacecraft.

2)   <u>After the LOI burn</u>; the spacecraft is already in a low orbit around the moon and return would simply involve pushing up the schedule of the Trans-Earth Injection (TEI) burn which has already been planned for earth return.

3) <u>During Lunar Descent (LD)</u>; the spacecraft would use available ΔV allotted for full LD and Lunar Ascent (LA) phases to return to Low Lunar Orbit (LLO) and initiate TEI burn for Earth return.

4) <u>After LA and LLO</u>; initiate TEI burn for Earth return as presented in cases 2) and 3) for a mission abort.

5) <u>After the TEI burn and before Earth re-entry</u>; as the mission has already been completed, the only fuel that remains is the small percentage of allowable fuel margin. The allowable fuel margin is presumably negligible; however, it could potentially be used to increase return velocity thereby reducing time to return, provided re-entry concerns are met.

It is for these aforementioned reasons that the scope of abort feasibility will be focused on the outbound lunar transit mission phase.

In the event of an emergency situation requiring an abort scenario there are two possible methods of return:

1) Do nothing; utilize the FRT which would presumably be planned into the mission as essential to crew safety.

2) Perform a direct abort; effectively halting the spacecraft and turning around to return to Earth, the astrodynamic equivalent of a U-turn, as shown in Figure 3.1.

The first option of abort via free return trajectory requires little study in regards to feasibility as it is a passive abort method requiring no trajectory

change maneuvers. In the case of a hybrid trajectory being utilized, as with Apollo, the hybrid trajectory would be designed with abort capabilities as a constraint.
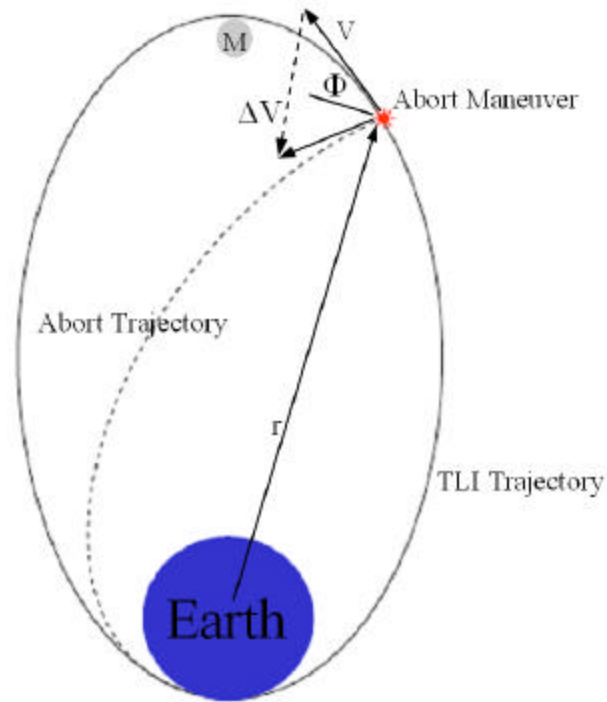
Figure 3.1 Direct abort trajectory

The second method of aborting a lunar mission via direct abort is the primary subject of the present study. In order to design for the possibility of a direct abort, a model needs to be created to study the method feasibility and requirements. The model should also be flexible so as to accept a wide variety of translunar trajectories such that any future missions can be examined.

Direct solution of the basic orbital equations served as a basis for the model rather than the patched conic method due to errors incurred in return

trajectory calculations. The patched conic method works well for outbound trajectories as when the primary gravitational force of the Earth is considered, the lunar gravitational force on the spacecraft is ignored. The magnitude of the Earth's gravitational force compared to the lunar gravitational force on the spacecraft makes this assumption an acceptable one. The patched conic method only considers the lunar gravitational force on the spacecraft when it is inside the lunar sphere of influence, at which point the Earth's gravitational field has a weaker effect. Problems arise in the return trajectory however when the inverse of the situation is utilized. When leaving lunar space, the gravitational force on the spacecraft from the Earth's influence compared to that of the Moon's is not a negligible factor. In this case the Earth's influence is simply too large to be ignored as in the case of ignoring the lunar gravitational influence for lunar bound trajectories. As the focus of this study is abort trajectories returning the spacecraft to Earth the errors incurred by utilizing the patched conic method on return trajectories prohibited the use of the method.

In creating an astrodynamic model two primary objectives must be addressed. First, the model must accurately track the trajectory. A translunar trajectory, as well as any orbital trajectory, can be defined by stipulating position and velocity. In the case of translunar trajectories, the obvious choice for trajectory definition is the altitude and final velocity at engine shut down following the translunar injection maneuver. From this point until injection into

low lunar orbit the ability to accurately determine abort feasibility is directly dependant on the ability to track the spacecraft's trajectory with accuracy.

The second of the primary objectives for the astrodynamic model is the determination of abort requirements. Any abort maneuver to place the spacecraft on a return to re-entry trajectory will have a defined ΔV requirement based on the current position and velocity of the spacecraft. In order to specifically define the regions of the translunar trajectory where a direct abort is feasible the required ΔV maneuver must be known at all points in transit on the translunar trajectory. By directly comparing the abort ΔV requirement with the propulsive capabilities of the CEV via various staging options across the translunar trajectory, the feasibility of a direct abort at any point during transit can be determined.

Once the available trajectory has been defined, tracked, and abort feasibility regions determined, a secondary objective for the astrodynamic model emerges. While it is known that at some intermediary region during the translunar trajectory the ΔV requirement for a direct abort will likely exceed the propulsive capabilities of the CEV, the converse is also true. It is not unreasonable to postulate that there will be regions where the direct abort ΔV requirement is less then the propulsive capabilities of the spacecraft. For these regions of direct abort feasibility it would be advantageous to ascertain the magnitude of the fuel margin in excess of the required ΔV for direct abort. The

excess fuel margin subsequent to abort would serve no purpose upon arriving at the re-entry corridor interface. Therefore it is desirable to attempt to utilize the excess fuel to attain a higher energy return trajectory; consequently a reduction in time of flight to return can be achieved. In an emergency situation requiring a direct abort, it is likely that any decrease in time to return would be beneficial to crew survivability.

3.2.   Trajectory Characterization

In order to more thoroughly define the abort feasibility envelope, possible lunar transfer orbits were modeled to provide a baseline. To characterize the possible lunar transition orbits, the Time Of Flight (TOF) was decided upon as the dominant metric. With the knowledge that a Hohmann transfer would have a transit TOF of 120 hours and that this is in general the lowest possible energy transfer, it set a bounds for the possible range.[16] Thus it was decided to evaluate the possible transfer orbits ranging from a TOF of 32 hours up to 120 hours for future missions. The lower bound of 32 hours is based upon the required TLI velocity to achieve such a short TOF. Not only is 11.2 kilometers per second a potentially prohibitively high ΔV, it represents the transition of lunar trajectories from elliptical to hyperbolic. Figure 3.2 illustrates the relationship between TLI velocity and its consequential TOF to lunar orbit.
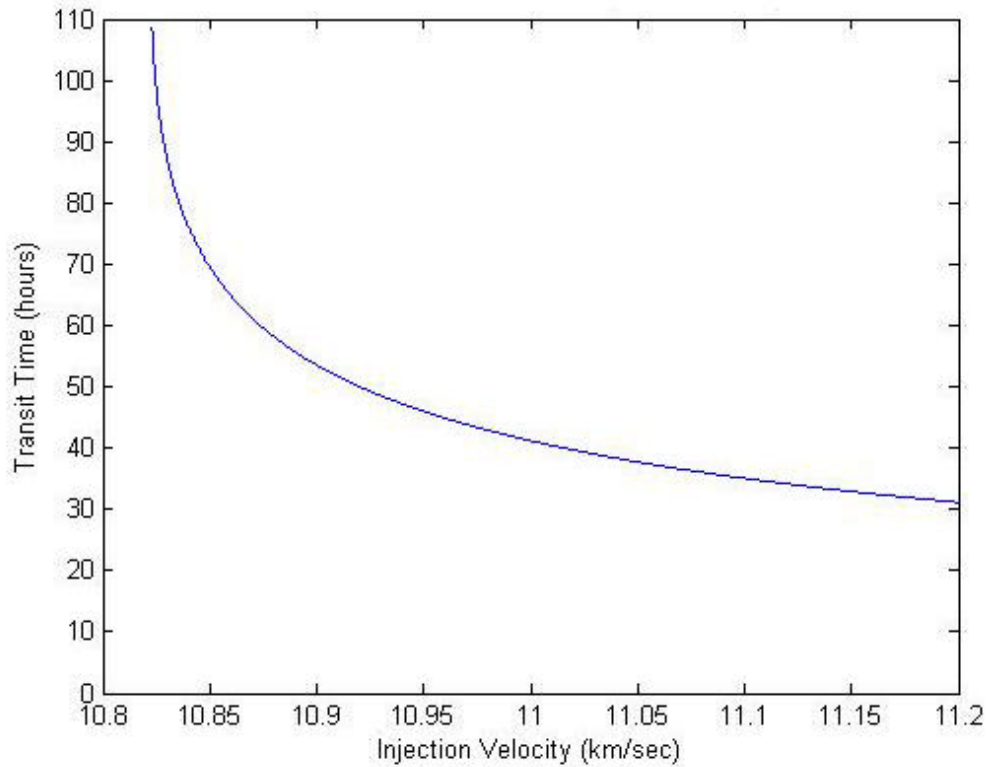
Figure 3.2 Transit time versus translunar injection velocity

Although not included in this present effort, higher energy transfers (TLI velocity greater than 11.2 km/s to reduce TOF further) could be accounted for by simply changing the bounds. Though it was presumed that due to the nature of the system the vast ΔV increase required for an almost trivial reduction in TOF does not justify the overall system mass increase to accommodate extra fuel. In addition transfer orbits in that high of an energy range transition to hyperbolic trajectories (eccentricity greater then 1) and would not be utilized on manned lunar missions. Once an eccentricity greater than 1 has been attained, the trajectory becomes hyperbolic and therefore providing escape velocity from

near-Earth space. Such a trajectory would never be utilized for a manned mission as a lunar orbit insertion maneuver propulsion failure would condemn the crew to drifting through deep space.

As previously mentioned, any orbit can be specifically defined by a position and velocity. In the case of this model, translunar injection conditions were selected as the initial trajectory definition parameters. Such trajectory definition is advantageous in specifying future missions as well as comparing with Apollo trajectory data since TLI conditions are of significant importance to be documented for any lunar mission. From the specified TLI conditions the trajectory in its entirety is charted via iterative solution of the basic orbital equations throughout the range of radii from TLI to LOI. The orbital energy equation (1)[16] is utilized, where e is the orbital energy, V is spacecraft velocity, r is radius, and m is the gravitational constant:

$$e = \frac{V^2}{2} - \frac{m}{r} = -\frac{m}{2a}$$ (1)

Also utilized was the angular momentum equation (2)[16], often applied to the law of conservation of angular momentum.

$$h = rv \cos \Phi$$ (2)

The flight path angle is defined as the angle measure between the velocity vector and the local horizontal plane which is defined as the plane normal to the radius

vector. Both these equations are utilized in conjunction with various forms of the

basic orbital geometric parameters:

$$r = \frac{p}{1 + e \cos \boldsymbol{n}} \tag{3}$$

$$e = \frac{c}{a} = \sqrt{1 + \frac{2\boldsymbol{e}h^2}{\boldsymbol{m}^2}} = \frac{r_a - r_p}{r_a + r_p} \tag{4}$$

$$p = a\left(1 - e^2\right) \tag{5}$$

$$r_p = \frac{p}{1 + e} = a(1 - e) \tag{6}$$

$$r_a = \frac{p}{1 - e} = a(1 + e) \tag{7}$$

$$p = \frac{h^2}{\boldsymbol{m}} \tag{8}$$

$$r_p + r_a = 2a \tag{9}$$

Equation (3) gives the radius for a specified true anomaly.[17]   While

equations (4) and (5) define the eccentricity and semi-latus rectum respectively.[18]

Equations (6) and (7) solve for the periapsis and apoaspsis radii respectively.[16]

Equation (8) gives a useful relationship between the semi-latus rectum and

angular momentum.[19] Finally, Equation (9) is a simple relationship between the

semi-major axis and the peri and apo-apsis radii.[16]

Utilizing the aforementioned equations the trajectory was iteratively

traced out based on radius. The radius vector was constructed by filling it with

the set data points utilized along the trajectory. The condition of building the

radius vector in an increasing fashion until a radius equal to that of the orbit of

the moon was used. Instead of defining a specified number of points along the

trajectory, an optimum number of data points would be generated based on the

shape and characteristic of the translunar trajectory. Equation (1) was solved to

result in velocity at the *i-th* radius data point. Next, equation (2) was solved for

the flight path angle at this *i-th* radius data point. Then the radius data point

corresponding to the '*i*+1' index was set via addition of either 1 or 100 kilometers

depending on the value of the flight path angle. Equation (1) could now be

solved again for the velocity at the new '*i*+1' radius index value yielding the

velocity at this new radius. Lastly, the flight path angle at the new '*i*+1' index

could be calculated via solution of equation (2) Vectors containing the velocity,

radius, and flight-path angle at each point along the trajectory were stored for

later usage.

Of important note is the subject of resolution. In order to maintain data

vectors of reasonable length, both for review purposes and also to keep

computational time to a minimum, the trajectory was broken into approximately

10,000 data point stations. These data points represent the actual evaluations of

potential abort trajectories initiated at each of these points. A compromise was

conceived between having enough data points to accurately and smoothly

represent the translunar trajectory space vs. an overly ambitious resolution

resulting in extensive computation times. A dual resolution scheme was

created. In close proximity to Earth the spacecraft has both high velocity and high angular velocity implying it will sweep across a large area in a short time and hence short distance of radii which is the iterative basis. Flight-path angles for this region of the trajectory remain small since the spacecraft is swinging around the Earth, while far away from Earth where the flight path angle is larger, velocity and flight path angle both have a relatively small change for larger changes in radius. The resolution was defined such that for flight-path angles less than 35 degrees the radius would be iterated by 1 kilometer, and once the flight path angle exceeded 35 degrees the radius would be iterated by 100 kilometers. A dual resolution afforded high accuracy where the orbital parameters varied strongly with iterated radius and sufficient accuracy where the orbital parameters varied weakly with iterated radius. Radius was iterated from TLI injection altitude up to 378,000 kilometers for the lunar orbit radius necessitating the resolution compromise. In this manner the entire translunar trajectory could be analyzed accurately and efficiently.

Radial distance is one basis for characterizing the position of the spacecraft along the translunar trajectory. Another, perhaps more useful basis for mission analysis, is that of time of flight. If a reference mission time is established to start zero hour at the completion of the translunar injection maneuver, location of the spacecraft in transit can quickly be determined by knowledge of how many hours have passed since the TLI. Intuitively this allows

easy reference for determining position along the translunar trajectory at the time of any emergency event. The time of flight basis is imposed upon the translunar trajectory via:

$$T = \sqrt{\frac{a^3}{m}}\left(\left(E - e\sin E\right) - \left(E_o - e\sin E_o\right)\right)$$ 10)

Where E is the eccentric anomaly as can be solved for by solution of equation (11):

$$\cos n = \frac{e - \cos E}{e\cos E - 1}$$ (11)

Finally, where the true anomaly, n, can be solved for from equation (3). Thus working backwards from true anomaly to the eccentric anomaly combined with the eccentricity from equation (4) yields a time of flight to reach the specified data point from the initial time of completion of the TLI maneuver. As a measure of clarification the eccentric anomaly, E, represents the value at the current data point. Where as the E_o eccentric anomaly represents the anomaly at the beginning of the segment of the trajectory currently under time of flight calculation. The time of flight is calculated as the time elapsed as the spacecraft travels from point E_o to point E. The returned time of flight unit is seconds, which is easily converted to hours, and stored in a time of flight vector characterizing the incremental flight times for each progressive data point in the translunar trajectory. The time of flight vector can be used to plot the trajectory from a basis of mission time.

42

3.3. *Direct Abort Required DV*

The feasibility for a direct abort is based upon a comparison of ΔV required for abort with the available ΔV from the mission allotted fuel plan. This available ΔV is calculated as part of an astrodynamic model based on transfer orbit energy levels planned for the mission. Due to the magnitude and orientation of the velocity vector at any given point along the lunar transfer orbit, there are three distinct regimes during the lunar transfer phase to be concerned with, as illustrated in Figure 3.3:

1)	Close to Earth the magnitude of velocity is very high, however the angle Φ it makes with the reference velocity vector (the reference velocity vector is normal to the radius vector) is small, thus ΔV required for a direct abort is small and the maneuver is feasible.

2)	At a defined mid-region of the transfer orbit, the magnitude of the velocity vector and its large value of Φ serve to make the required ΔV for a direct abort prohibitively high.

3)	Close to the moon the magnitude of the velocity vector is low, and the angle Φ is also once again small, allowing for direct abort feasibility.
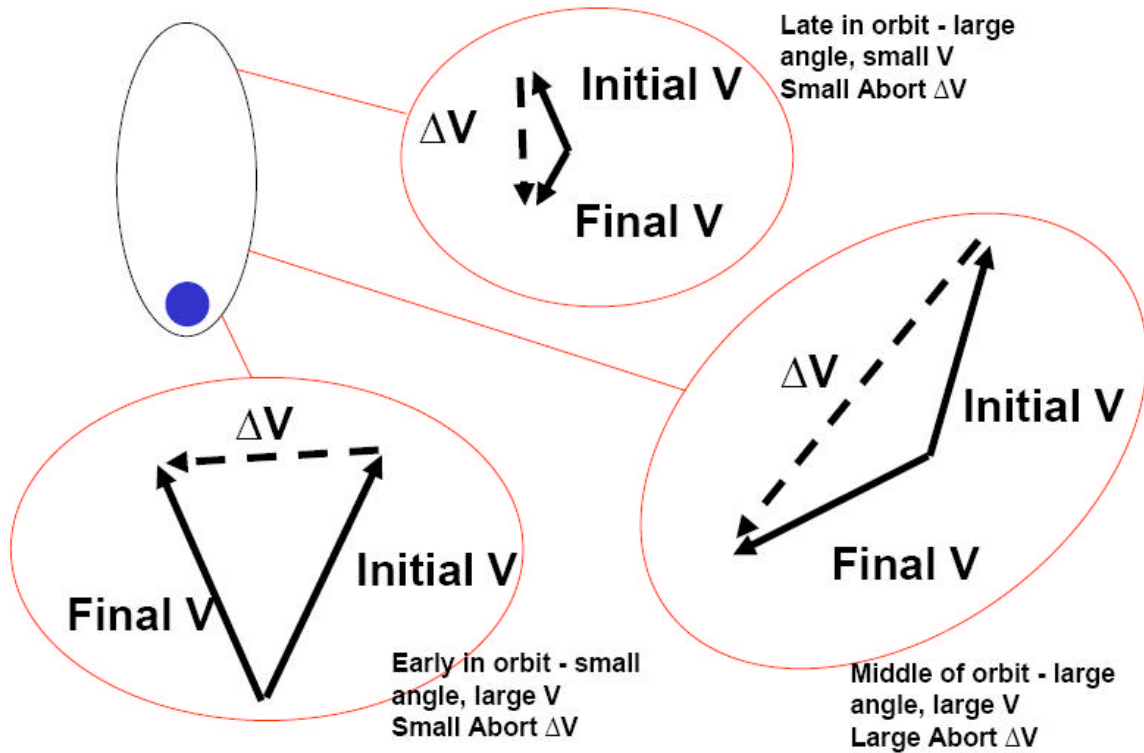
Figure 3.3 Required ΔV maneuvers for direct abort

The basic approach is to "reflect" the spacecraft's current velocity vector back to Earth if possible utilizing available fuel. The ΔV required for this maneuver is based on velocity and flight path angle, and is characterized by[20]:

$$\Delta V = 2V \sin \Phi \qquad (12)$$

Next a calculation of available ΔV for a direct abort is required. ΔV for each segment of the mission is calculated from each specific TLI trajectory analysis, while ΔV for the lunar descent and lunar ascent are also based from a reference orbit of 100 km above the moon, as this is likely to be the parking orbit for the CEV during lunar missions.[21] It also should be noted that the ΔV for lunar descent and lunar ascent is calculated based on total vehicle mass at the time of

abort burn, such that the ΔV for lunar descent module is normalized to the entire vehicle via mass ratio estimations even though the actual fuel budgeted is for descent of lunar module only. Reducing this budgeted ΔV amount by the mass ratio between the module and the entire spacecraft yields the effective ΔV for the specific module. An important during the abort staging tradeoff analysis and can be accomplished via equation (13):

$$\Delta V_{Effective} = \Delta V_{\text{mod}\, ule}\left(\frac{M_{total\_spacecraft}}{M_{design}} \right) \tag{13}$$

Where the mass of the total spacecraft in its current configuration, over the mass of the module's designed propulsion system capabilities completes the mass fraction. The effective ΔV for each stage can then be calculated based on adjusted mass fractions depending on staging methods. Once the effective ΔV has been calculated for each module, the total available ΔV for the direct abort can be calculated by the following equation (14):

$$\Delta V_{Available} = \sum_{Initial\_stage}^{Final\_stage} \Delta V_{Effective} \tag{14}$$

The available ΔV of the spacecraft can now be directly compared to the ΔV required for a direct abort to determine feasibility of an abort at any point along the translunar trajectory.

Chapter 4.   Optimization of Return Trajectories

Once the ΔV requirement for a direct abort has been determined via the methods described in Chapter 3, it is desirable to efficiently utilize any fuel left after the direct abort to accelerate the crews return. The first half of this chapter involves optimization for the expediting return, while the second half explains the multi-segmented pseudo-direct abort trajectory optimization scheme.

4.1.   Expedited Return in Feasible Region

The region of the translunar trajectory in which a direct abort is feasible can now be specifically defined, by the aforementioned model, as well as characterizing available and required ΔV's for such a maneuver. At the boundary of this region the available ΔV from the spacecraft is equal to the required ΔV for the abort maneuver. However, after this region there exists an excess fuel margin where there is more available ΔV then required for the abort maneuver. Therefore, there may be an advantage available in the form of excess fuel to speed the return to Earth on a higher-energy trajectory. Ideally, all excess fuel would be used to attain a higher energy return orbit; contingent upon matching re-entry corridor conditions. The conditions used here were based on flight data from Apollo 4, with a re-entry velocity of Mach 40. This was perceived as the highest velocity to safely return the crew, and was considered

valid due to its basis on actual flight data. This limit can be easily changed if the CEV can withstand higher re-entry Mach numbers based on heating rates and G-force limits imposed by flight path angle constraints.

It may be therefore desirable to utilize this excess fuel to enable a higher energy return transfer orbit in order to reduce the time of flight to re-entry for the spacecraft.

4.1.1. Methodology/Algorithm

The first design iteration of the expedited return method was founded on the law of conservation of angular momentum. The excess fuel was divided into two discrete burns, one at the point of abort, and one just prior to reaching the re-entry corridor interface. The first burn at the position and time just after the abort maneuver could in practice be combined with the abort burn to reduce the number of engine firings, however for calculation purposes was taken to be a separate burn. This would inject the spacecraft onto a higher energy trajectory towards Earth. The second burn in close proximity to Earth would be required to reduce the energy level of the transfer such that the re-entry trajectory could satisfy re-entry velocity and flight-path angle constraints. The fuel margin was divided by the ratio of radii for each burn position. In effect this ensured that the exact amount of angular momentum imparted onto the spacecraft during injection into the higher energy transfer would be subtracted from the spacecraft

to allow compliance with re-entry constraints. Otherwise re-entry velocities would far exceed tolerances.

4.1.2. Implementation

The final design iteration of the algorithm is similar in technique, preserving the dual burn mode, however it employs a gradient based optimization scheme. The optimizer was allowed to vary design variables of the two ΔV magnitudes, the re-entry velocity and re-entry flight-path angle. Constraints on maximum re-entry velocity and a plus or minus one degree margin on flight-path angle were imposed. Studies from the Apollo missions found that a one degree variance in re-entry flight path angle had minor effects on re-entry heating and g force loading and consequently minor effects on abort trajectories initiated from distances greater then a few Earth radii.[22] The effect of the flight path angle can be seen in Figure 4.1 as it defines the re-entry corridor for the Apollo mission. Due to similarities in design and proposed lift to drag ratio of the CEV, the corridor is just as applicable today as it was for the Apollo missions.
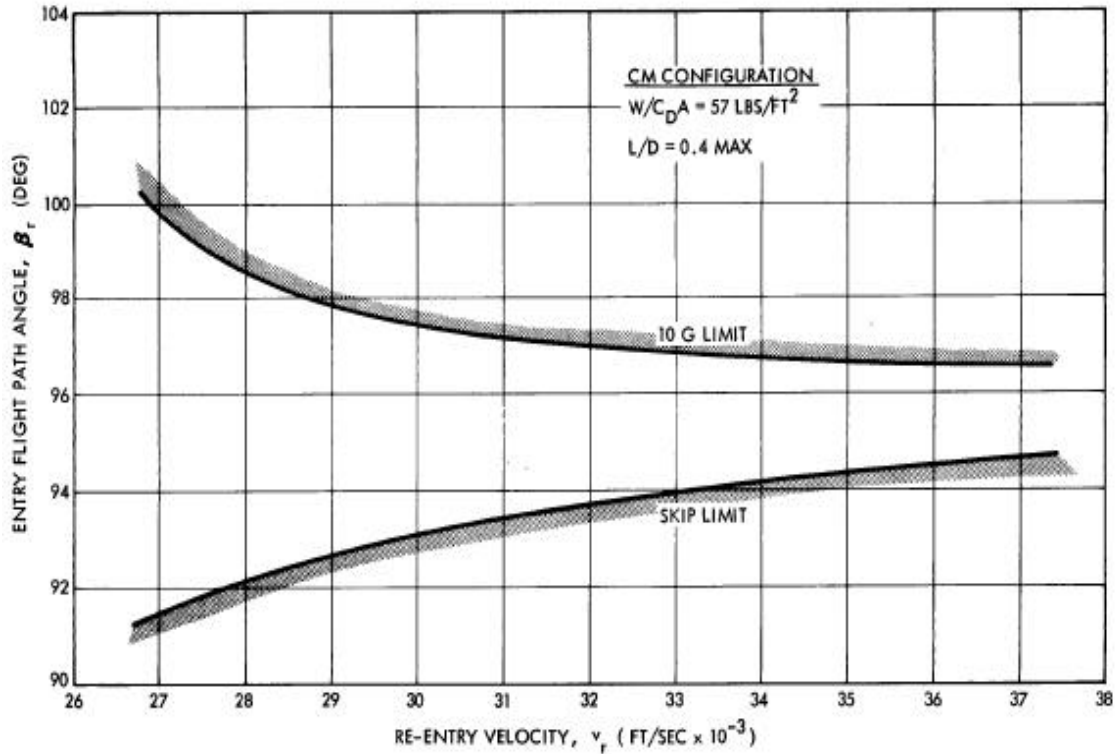
Figure 4.1 Constraints on flight path angle forming re-entry corridor[22]

The Sequential Quadratic Programming (SQP) optimization scheme returns burn data as well as time of flight for the new higher energy trajectory. First a function was created for use by the main program. This function called the optimization scheme and contains radius, velocity, and flight path angle data at the specified trajectory data point, as well as the available ΔV for optimization. It is important to note that the ΔV available for the optimization scheme is the difference between the total effective ΔV of the spacecraft based on a specified abort staging method and the required ΔV for the abort maneuver. In this fashion, only the excess fuel not required for the direct abort was available to the

optimizer. Table 4.1 outlines the design variables, and their respective imposed constraints, the SQP optimization scheme had control of.

Table 4.1 Direct abort fast return optimization design variables

Variable	Description	Constraint
r	Radius (Position)	Equality (Fixed Value)
V	Velocity	Equality (Fixed Value)
Φ	Flight Path Angle	Equality (Fixed Value)
ΔV Available	Available Fuel to Optimize	Equality (Fixed Value)
$\Delta V1$	Accelerating Burn	$\Delta V1 + \Delta V2 <= \Delta V$ Available
$\Delta V2$	Decelerating Burn	$\Delta V1 + \Delta V2 <= \Delta V$ Available
Φ_{re}	Re-Entry Flight Path Angle	$-7.5° < \Phi_{re} < -5.5°$
M_{re}	Re-Entry Mach Number	Maximum 40

The first four variables are locked as constants via equality constraints. While this process appears counter intuitive to the very nature of a variable, it was required as exact position and velocity data as well as available fuel for optimization are required inputs for the objective function. The rest of the variables are bounded by simple linear constraints. A nonlinear constraint function based on conservation of angular momentum was also imposed to relate and compliment the energy gained by the accelerating burn to that of the energy diminished by the decelerating burn. The objective function for minimization is the time of flight function, in this manner the SQP optimizer returns the optimum division of the available fuel to affect the fastest possible return bounded by the fuel and re-entry corridor constraints. The division of available fuel and the resulting time of flight are returned for each data point in the abort feasibility region along the outbound translunar trajectory.

Tracked across the entire direct abort feasibility region it profiles fastest returns possible from any point in the lunar trajectory, allowing a significant reduction in return time if utilized. Any reduction in return time, depending on the emergency situation requiring a mission abort, could translate into increased crew survivability.

4.2. Infeasible Region Trajectory Search

Now that the region of direct abort feasibility can be characterized a region of abort infeasibility emerges. In this region the required ΔV for a direct abort is prohibitively high. The obvious option is simply to wait until the spacecraft crosses the threshold into the direct abort feasibility region and proceed with an abort maneuver. While required ΔV in the peak of infeasibility can be quite high, reaching up to the 10 kilometer per second range, near the boundaries of the region it is not nearly as high. These boundary regions warrant closer examination as to possible trajectory options. If successful, any abort trajectories found in these boundary regions would serve to reduce the duration of the infeasibility region, thereby increasing abort options for the spacecraft and consequently crew survivability in the event of an emergency.

4.2.1.　　Methodology/Algorithm

Since a reflected orbit direct abort method is already found to be a nonviable option in this region a new concept of a pseudo-direct abort was devised. The pseudo-direct abort would in effect turn the spacecraft around onto a return trajectory via the utilization of an intermediary trajectory. By allowing multiple trajectory segments, a small ΔV maneuver could be performed. The spacecraft could then coast along an intermediary trajectory until a position and velocity is attained that would have a feasible direct abort solution. Figure 4.2 illustrates the differing strategies of a single burn direct abort, and a dual burn pseudo-direct abort.
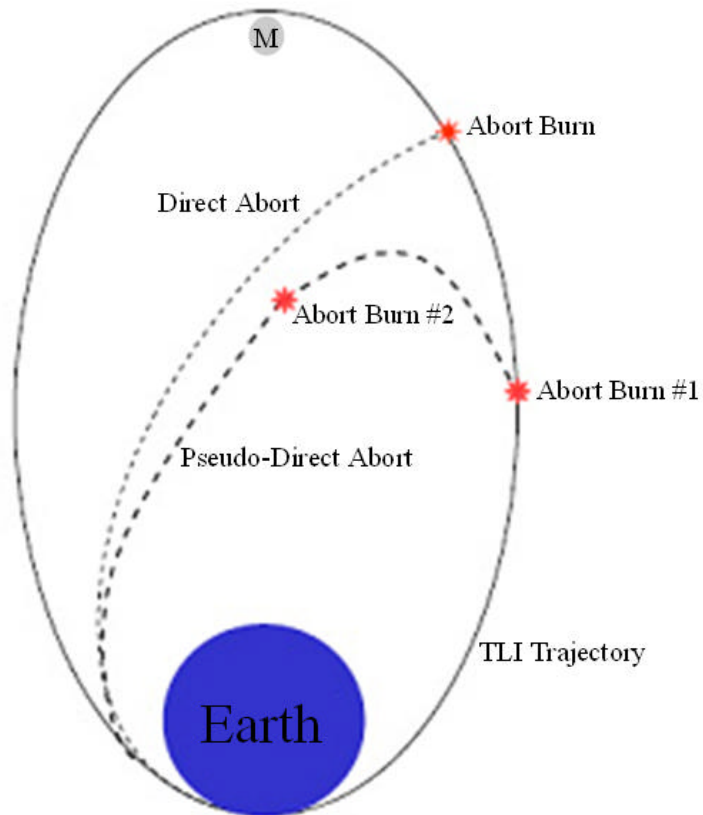
Figure 4.2 Dual burn pseudo direct abort versus direct abort

Due to the nature of the pseudo-direct abort problem, it is a situation ideally suited for optimization. By allowing the optimizer to vary the design variable of ΔV and coast time for each trajectory segment, the optimizer is put in a position to find any feasible trajectories. The optimizer searches the design space in an effort to search the direct abort infeasible region for any unconventional trajectories not obvious to the operator. The optimization scheme, the same gradient based SQP method previously used, would again be constrained by re-entry corridor conditions.

4.2.2.   Implementation

Although originally intended to become an added function to the existing astrodynamic model, as in the case for the feasible abort region optimizer, this pseudo-direct abort scheme proved impossible to integrate. The solution became the development of an entirely separate astrodynamic model specifically constructed for the pseudo-direct abort problem.   An iterative solution of the equations of motion via an Ordinary Differential Equation (ODE) solver became the foundation for the new model.

The numerical integration via the ODE solver utilized an x vector:

$$x = \begin{Bmatrix} X \\ Y \\ V_x \\ V_y \end{Bmatrix} \tag{15}$$

where the Cartesian position co-ordinates are defined by the components of the radius vector and the Cartesian velocity components are determined by velocity vector components.   The velocity vector components are found from the combination of the velocity magnitude and the flight path angle solved through simple sine and cosine trigonometric relations. The x vector is then input into a derivative function which returns the derivative vector defined by:

$$dx = \begin{Bmatrix} V_x \\ V_y \\ a_x \\ a_y \end{Bmatrix} \qquad (16)$$

For clarity purposes the equations for a_x and a_y are defined in equations (17) and (18) respectively, for brevity position terms have been abbreviated by a subscripted 'p':

$$a_x = \left[\frac{-\boldsymbol{m}}{\left[\sqrt{X^2 + Y^2} \right]^3} \right] X \qquad (17)$$

$$a_y = \left[\frac{-\boldsymbol{m}}{\left[\sqrt{X^2 + Y^2} \right]^3} \right] Y \qquad (18)$$

Finally the x and dx vectors can be input into the ODE solver along with the desired coast time increment to acquire the position and velocity data at the optimizer specified coast time. The position and velocity data at this point represent the position of the ΔV maneuver utilized to inject the spacecraft onto the next trajectory segment.

ΔV engine burn magnitudes as specified by the optimizer came in the form of a set of x direction component and y direction components of the ΔV. Equations (19) and (20) show the resulting simple addition method of analytically performing an engine burn:

$$V_{x,i+1} = V_{x,i} + \Delta V_x \qquad (19)$$

$$V_{y,i+1} = V_{y,i} + \Delta V_y \qquad (20)$$

55

The '*i*' index representing the spacecraft velocity components at the completion of the specified coast time, and the '*i*+1' index of course representing the new spacecraft velocity components at the start of the new trajectory segment. The new velocity data combined with the position at completion of the coast time are combined to form the *x* vector for the next trajectory segment. In this manner the entire process can be iterated from the beginning, starting with the new found *x* vector, for the addition of subsequent pseudo-abort trajectory segments.

Due to the complexity of tracking up to several trajectory segments and matching them up to create a complete closed trajectory from abort point to re-entry; it was deemed necessary to work backwards since the terminal state was explicitly specified at re-entry. Starting with re-entry corridor conditions, a trajectory segment was traced by iteratively tracking position and velocity data up to a specified coast time. The equations of motion are iterated along this segment and solved for by the ODE solver. Once the coast time on the first trajectory segment is attained, a ΔV maneuver is performed. The ΔV maneuver injects the spacecraft onto a new trajectory segment along which position and velocity are tracked again via ODE solutions of the orbital equations of motion until the optimizer specified coast time is reached. A complete trajectory could be built up in reverse, composed of anywhere from two to four segments. The final trajectory segment would have a coast time calculated based on matching the position of the spacecraft at abort, and a final ΔV maneuver was calculated to

match the pseudo-abort trajectory set to the outbound translunar trajectory. When the data set is reversed a sequence of ΔV maneuvers and coast times is presented in correct abort sequence order, forming the pseudo-direct abort trajectory.

Inherent to the pseudo-direct abort problem is a question of optimum segments in the complete trajectory. A direct solution of this would require a secondary optimizer to determine and input the ideal number of trajectory segments. Thus the model was set up with number of segments as an input variable. This allowed a parametric study of two, three, or four segmented pseudo-direct aborts. Pseudo-direct abort trajectories were limited to four or less segments out of a desire to minimize the number of mid course corrections requiring engine start up because of reliability concerns during an emergency situation.

Table 4.2 lists the various design variable fed into the SQP optimizer:

Table 4.2 Pseudo-direct abort optimization design variables

Variable	Description	Constraint
r	Radius (Position)	Equality (Fixed Value)
V	Velocity	Equality (Fixed Value)
Φ	Flight Path Angle	Equality (Fixed Value)
ΔV Available	Available Fuel to Optimize	Equality (Fixed Value)
Φ_{re}	Re-Entry Flight Path Angle	$-7.5° < \Phi_{re} < -5.5°$
M_{re}	Re-Entry Mach Number	Maximum 40
	Repeated Variables per Trajectory Segment	
T	Coast Time	Maximum Infinity
ΔVx	Delta V maneuver X direction	(+) or (-) Infinity
ΔVy	Delta V maneuver Y direction	(+) or (-) Infinity

The first six design variables are same as the design variables for the first optimization, minus the two ΔV maneuvers. For the pseudo-direct abort optimization, instead the cost time and each component of the ΔV maneuver are repeated variables. By this it is meant that the repeated variables are set sequentially for each trajectory segment. In this manner the number of design variables varied depending on the selected number of pseudo-direct abort trajectory segment. The total number of variables is simply six plus three times the number of trajectory segments. Such that two segments yields 12 variables, three segments yield 15 variables, and four segments yield 18 variables. The expandable method of design variable vector definition lends itself towards an unending supply of possible segments for a pseudo-direct abort. This flexibility allows more than four segments to be studied if it is deemed beneficial to utilize that many engine burn maneuvers. Conversely, model validation was enabled

by this flexibility, in that if a single trajectory segment is input the design variable vectors are set up to emulate a direct abort.

Due to required computation time for an ODE based objective function to the optimization scheme the entire region of direct abort infeasibility was not analyzed. Instead a sample data set of points along the trajectory in the direct abort infeasibility region was selected. From these points, current spacecraft telemetry could be input as well as the number of desired segments in the pseudo-direct abort trajectory. If a complete closed trajectory was found, a complete trajectory profile was returned. The profile includes position, velocity, ΔV, and coast time data for each trajectory maneuver.

Chapter 5.   Translunar Trajectory Analysis

The development of the model and implementation of optimization schemes described in the two preceding chapters allows a complete trajectory analysis as described in this chapter. A reference trajectory is chosen as a basis of comparison between the Apollo and CEV spacecrafts. This reference trajectory is utilized throughout the analysis such that the abort feasibility profile is presented, followed by the optimized expedited return and pseudo-direct abort analysis.

5.1.   Reference Translunar Trajectory

Throughout the creation of the model, the key goal was flexibility to allow for calculation of abort feasibility envelopes for any trajectory the CEV or other manned lunar missions may use. In order to set a basis common to the trajectory analysis, a single translunar trajectory across the analysis was utilized. The Apollo XV mission trajectory was chosen from Table 5.1.[23] The primary values utilized were the translunar injection altitude and final velocity which convert to 321.7 kilometers and 10.845 kilometers per second respectively. These values were used throughout the trajectory analysis for both feasibility determination and optimized utilization of any excess fuel, as well as for the optimized trajectory search centered on the region of direct abort infeasibility.

Table 5.1 NASA historical translunar injection flight data

Translunar Injection

	Apollo 11	Apollo 12	Apollo 13	Apollo 14	Apollo 15	Apollo 16	Apollo 17
GET	002:50:13.03	002:53:13.94	002:41:47.15	002:34:33.24	002:56:03.61	002:39:28.42	003:18:37.64
KSC Date	16 Jul 1969	14 Nov 1969	11 Apr 1970	31 Jan 1971	26 Jul 1971	16 Apr 1972	07 Dec 1972
GMT Date	16 Jul 1969	14 Nov 1969	11 Apr 1970	31 Jan 1971	26 Jul 1971	16 Apr 1972	07 Dec 1972
KSC Time	12:22:13 p.m.	02:15:13 p.m.	04:54:47 p.m.	06:37:35 p.m.	12:30:03 p.m.	03:33:28 p.m.	03:51:37 a.m.
Time Zone	EDT	EST	EST	EST	EDT	EST	EST
GMT Time	16:22:13	19:15:13	21:54:47	23:37:35	16:30:03	20:33:28	08:51:37
Altitude (ft)	1,097,229	1,209,284	1,108,555	1,090,930	1,055,296	1,040,493	1,029,299
Altitude (n mi)	180.581	199.023	182.445	179.544	173.679	171.243	169.401
Earth Fixed Velocity (ft/sec)	34,195.6	34,020.5	34,195.3	34,151.5	34,202.2	34,236.6	34,168.3
Space-Fixed Velocity (ft/sec)	35,545.6	35,389.8	35,538.4	35,511.6	35,579.1	35,566.1	35,555.3
Geocentric Latitude (deg N)	9.9204	16.0791	-3.8635	-19.4388	24.8341	-11.9117	4.6824
Geodetic Latitude (deg N)	9.983	16.176	-3.8602	-19.554	24.9700	-11.9881	4.7100
Longitude (deg E)	-164.8373	-154.2798	167.2074	141.7312	-142.1295	162.4820	-53.1190
Flight Path Angle (deg)	7.367	8.584	7.635	7.480	7.430	7.461	7.379
Heading Angle (deg E of N)	60.073	63.902	59.318	65.583	73.173	59.524	118.110
Inclination (deg)	31.383	30.555	31.817	30.834	29.696	32.511	28.466
Descending Node (deg)	121.847	120.388	122.997	117.394	108.439	122.463	86.042
Eccentricity	0.97696	0.96966	0.9772	0.9722	0.9760	0.9741	0.9722
C3 (ft^2/sec^2)	-14,979,133	-19,745,586	-14,814,090	-18,096,135	-15,643,934	-16,881,439	-18,152,226

5.2.   Translunar Abort Feasibility

5.2.1.   Apollo Spacecraft

Once a mission trajectory is chosen it can be input into the model for analysis.   In the event of an emergency situation, the first objective is determining available options.   Characterization of abort feasibility across the entire translunar trajectory allows an easy reference for determining if a direct abort is feasible.   Figure 5.1 shows the feasibility profile for the Apollo XV mission utilizing the nominal abort method as a function of altitude.
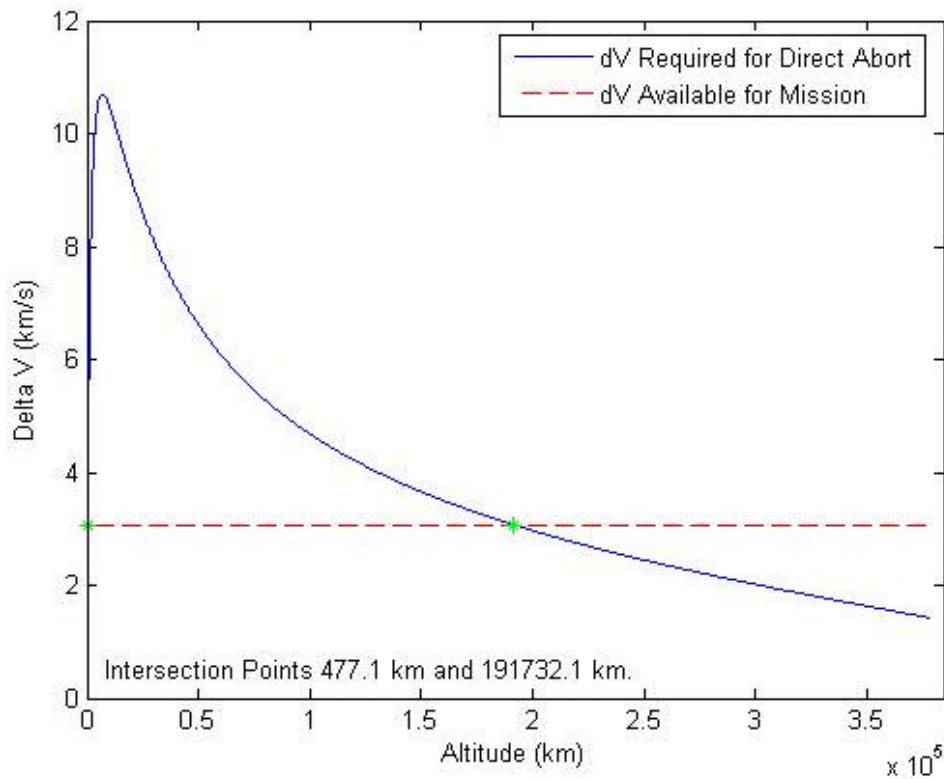
Figure 5.1 Apollo XV feasibility profile for nominal abort (altitude)

From the figure it is not readily clear that there are in fact two regions of abort feasibility. The first feasibility region is very small due to close proximity of the space craft to Earth, the velocity magnitude is very high as well as the rate of change of flight path angle. Figure 5.2 shows the first feasibility region on a much smaller scale for illustration purposes. The second region of feasibility is clearly recognizable as approximately the last 60% of the distance to the moon where the available ΔV exceeds the required ΔV for a direct abort.
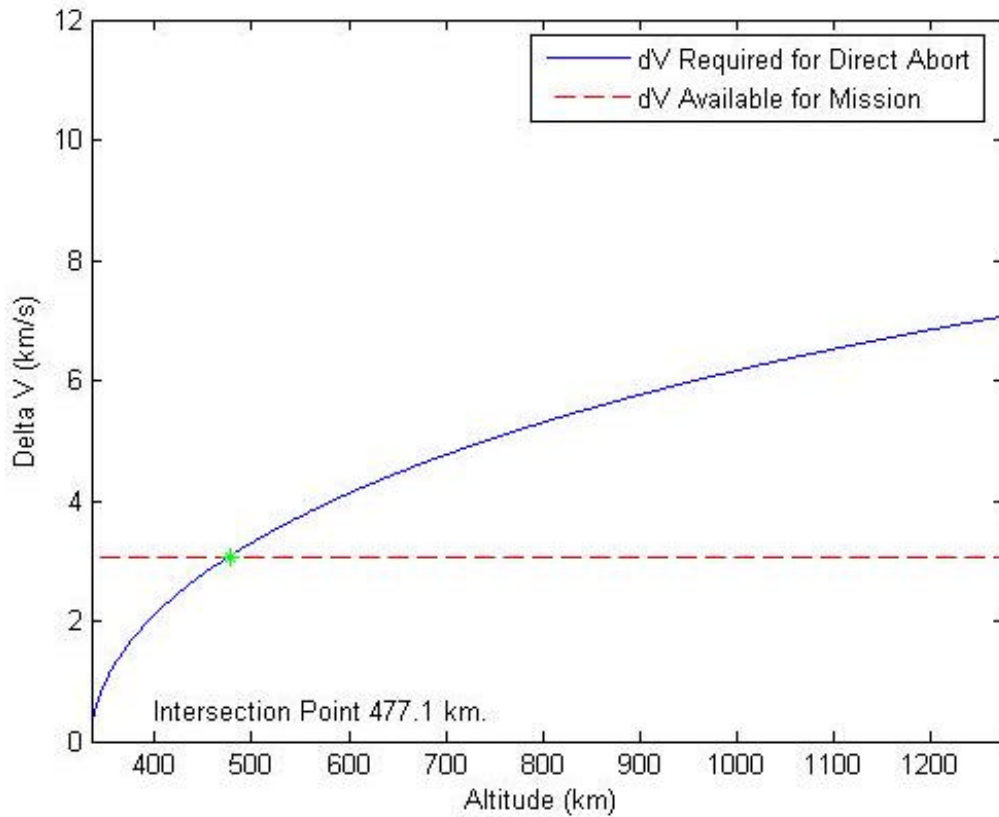
Figure 5.2 Apollo XV First Feasibility Region

As shown in the Figure 5.3, the magnitude of the abort infeasibility region

is approximately 22 hours, for a nominal abort, of the total three day journey.
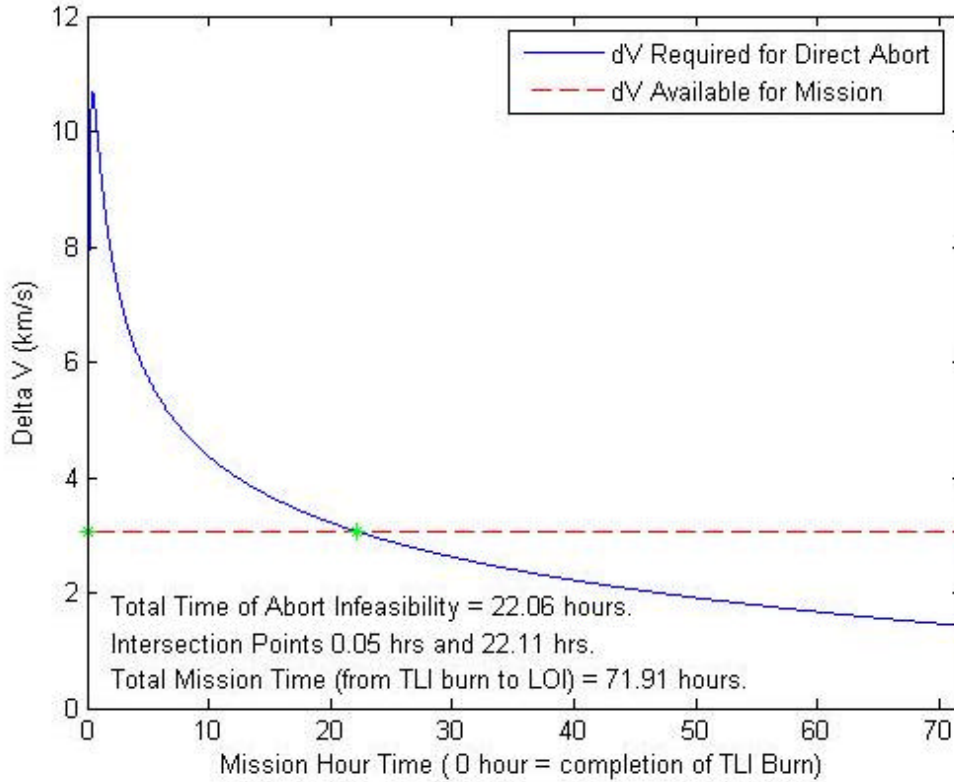
Figure 5.3 Feasibility profile for Apollo XV nominal abort (time)

The scale of hours from initial translunar injection is perhaps most

beneficial in an emergency situation. By tracking the course of the trajectory it

can easily be determined via inspection of the plot if the direct abort option is

feasible.

One conclusion to be drawn from the first feasibility region is that the

initial boundary is extremely soon after the TLI burn, on the order of five

minutes or less. Thus the time required for an abort decision and execution

extremely critical and in all likelihood prohibitively so. The abort procedure for the Apollo program in the event of a service module propulsion failure at lunar orbit insertion specifically built in a range of two to four hours for lunar module propulsion burn preparation.[8] Although technology has afforded vast increases in computational power, ground control as well as flight hardware, and guidance, navigation and control, it would seem unreasonable to presume that the decision and execution of a direct abort for the CEV could be completed in that short a time frame. Leading to the conclusion that if an emergency situation arises during that time the best option would be to wait until the boundary of the feasibility region has been reached and then perform a direct abort. It quickly becomes obvious why the reduction of the infeasibility region via increasing effective ΔV is beneficial.

The second conclusion to draw from the feasibility profile is the general trend. Inspection of the plot reveals that due to the required ΔV curve flattening out, that below about 5 kilometers per second of required ΔV, any small gain in propulsive capability can result in a significant reduction in the magnitude of the infeasibility region. However, since the required ΔV can reach a peak of ten km/s or more, it is not likely to ever completely reduce the infeasibility region.

A significant improvement can be achieved via used of the various abort methods to gain effective ΔV benefits. Figure 5.4 shows the effect of the staging methods on the abort feasibility profile for the Apollo XV mission.
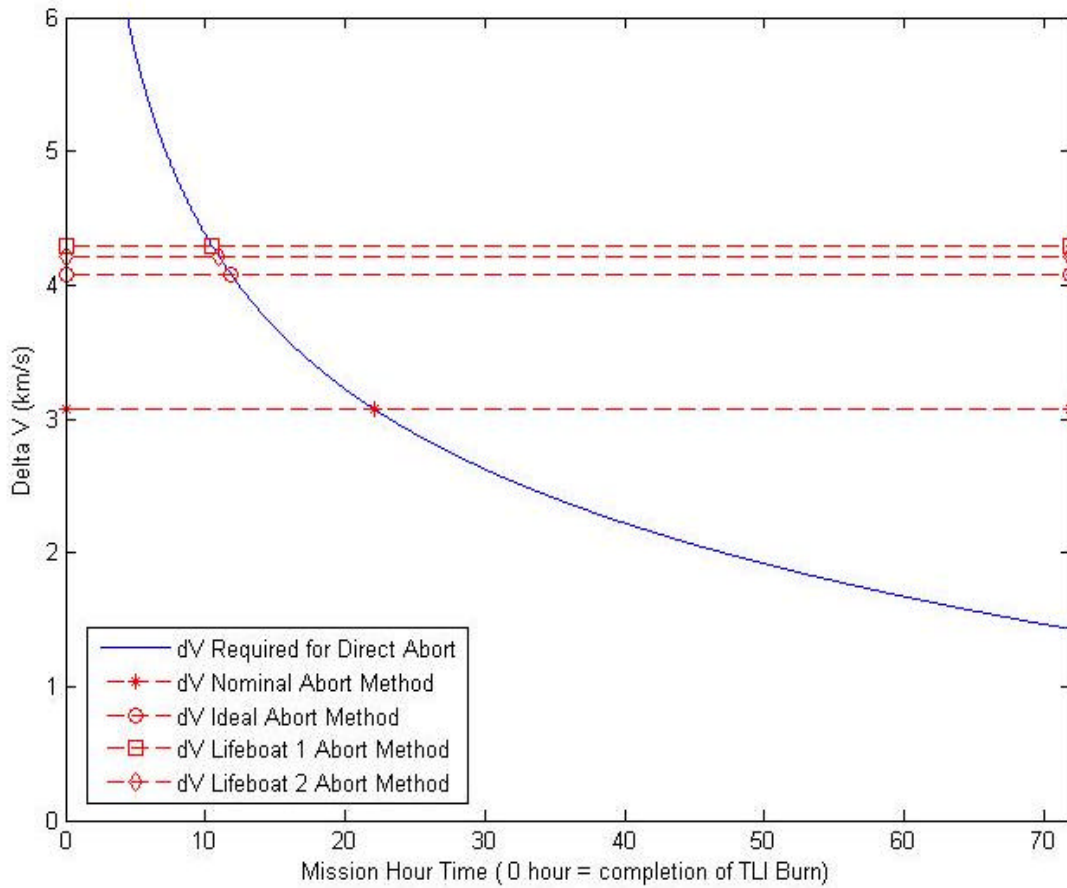
Figure 5.4 Feasibility profiles for various abort methods for Apollo XV

The benefits for the different staging methods show significant improvement over the nominal staging method. Though they fall close to one another, the lifeboat case 1 is clearly the most beneficial in terms of effective ΔV, followed by the second lifeboat method and the ideal abort method respectively. When compared in this manner the aforementioned trend of reduction in magnitude of the infeasibility region via increase in effective ΔV is readily apparent.

The effective ΔV's and corresponding direct abort infeasibility regions are summarized in Table 5.2.

Table 5.2 Apollo abort methods infeasibility region data

Method	Effective Delta V (km/s)	Infeasibility Region Data (hrs)		
		Duration	1st Boundary	2nd Boundary
Nominal	3.075	22.02	.05	22.08
Ideal	4.080	11.76	.07	11.85
Lifeboat 1	4.297	10.38	.07	10.46
Lifeboat 2	4.213	10.89	.07	10.98

In a worst case emergency situation, the maximum effective ΔV for the Apollo spacecraft and Apollo XV mission trajectory could be increased by 40% via the lifeboat 1 abort method. The lifeboat 1 staging method takes advantage of the best achievable mass ratios to affect a better effective ΔV, reducing the infeasibility region by 53%.

If an emergency occurred immediately following the translunar injection burn, the spacecraft would need to coast until direct abort becomes feasible. Therefore, for an emergency occurring inside the infeasibility region, the maximum time to return to re-entry would be 10.38 hrs multiplied by two (once to coast out, once for the return flight) or 20.76 hours. For an emergency occurring in the direct abort feasibility region the return to re-entry time is the same amount of time as the time between TLI and the abort burn. The coincidence in time of flight to return is due to simply reflecting the trajectory for return to Earth, time of flight remains the same as the original lunar bound trajectory.

68

5.2.2. CEV Spacecraft

As the concepts of the feasibility and infeasibility regions have been discussed in the Apollo example section, Figure 5.5 characterizes the abort feasibility profile for the CEV spacecraft. Also, as previously explained the mission trajectory utilized was that of the Apollo XV to allow direct comparison. Due to scale again the first feasibility region is not visible on Figure 5.5, but can be viewed in Figure 5.6.
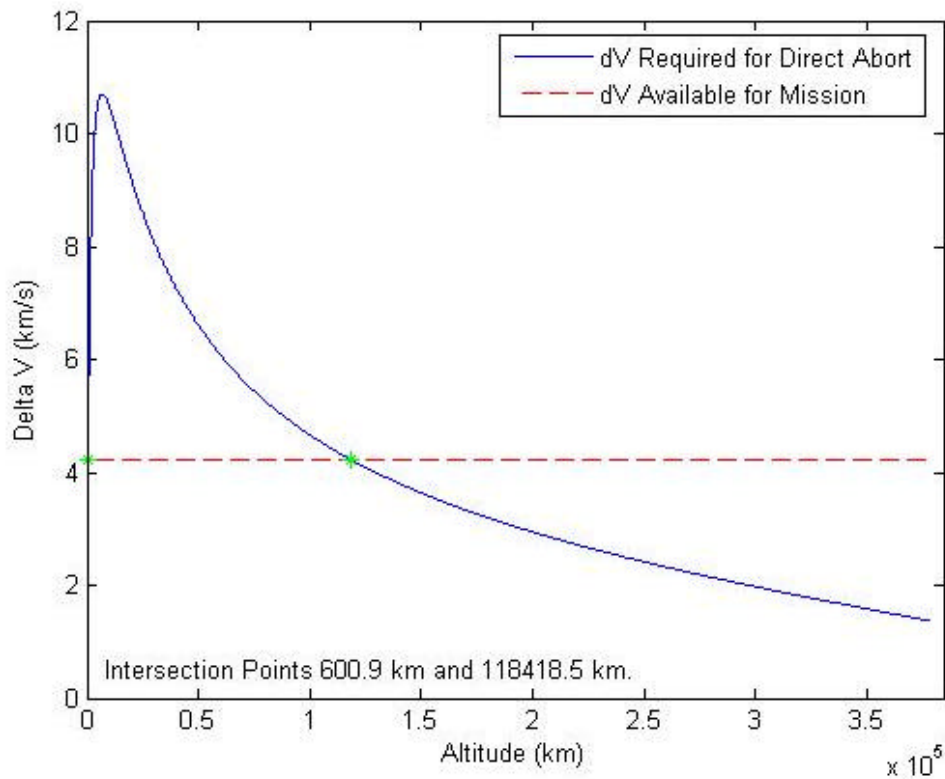
Figure 5.5 Feasibility profile for CEV nominal abort (altitude)
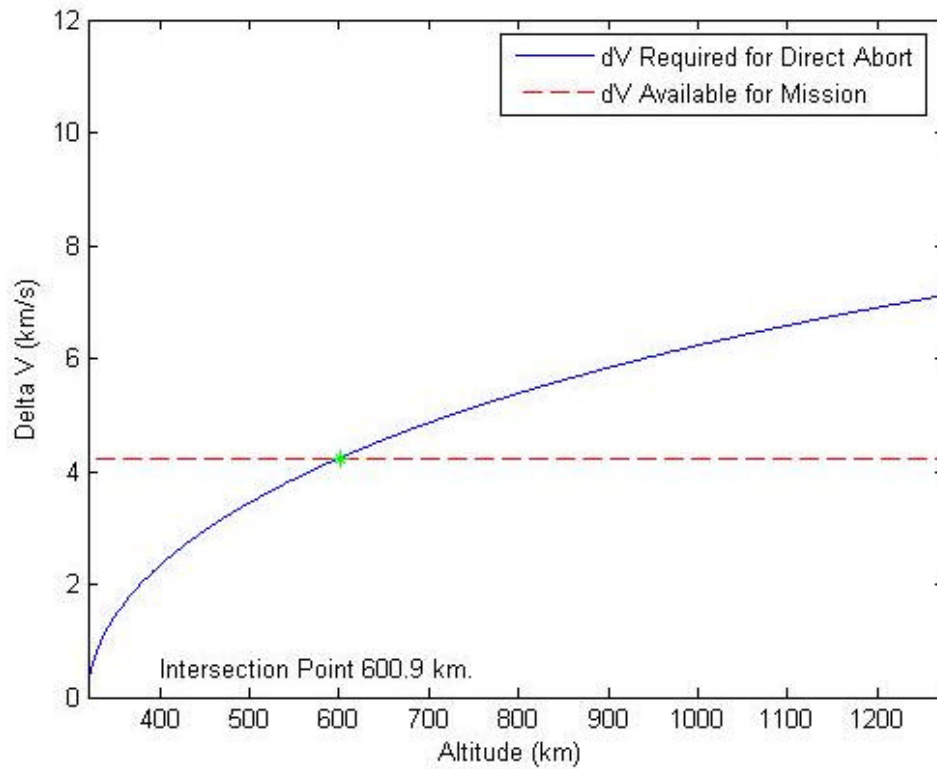
Figure 5.6 CEV first feasibility region

Figure 5.7 illustrates an already much smaller infeasibility region then the Apollo spacecraft; only 10.75 hours. Again this is for the nominal case so given the ideal abort method, one can expect an even further reduced infeasibility region.
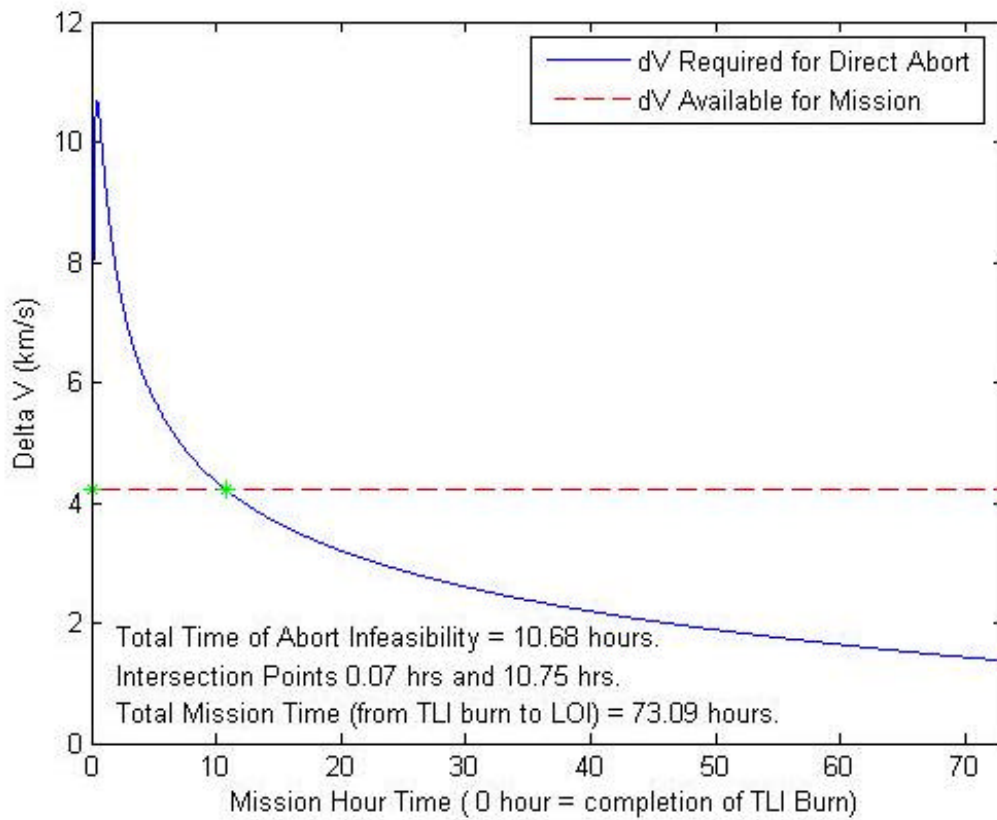
Figure 5.7 Feasibility profile for CEV nominal abort (time)

The various effective ΔV's for the different methods are displayed in Figure 5.8. For the CEV the ideal abort method achieves the shortest infeasibility region, or conversely the largest feasibility region. The lifeboat 1, nominal, and lifeboat 2 methods follow in that order respectively. Of interesting note is that the lifeboat case 2 is actually detrimental to the cause of increasing abort feasibility. The reasoning for this detrimental impact is due to the nature of the CEV, as its design criteria focuses on a large lunar module to affect longer duration missions as well as full crew complement to the lunar surface. Based on

the design criteria the lunar module has grown significantly in mass from the Apollo spacecraft counterpart, offsetting the mass ratio benefit designed into the lifeboat abort methods.
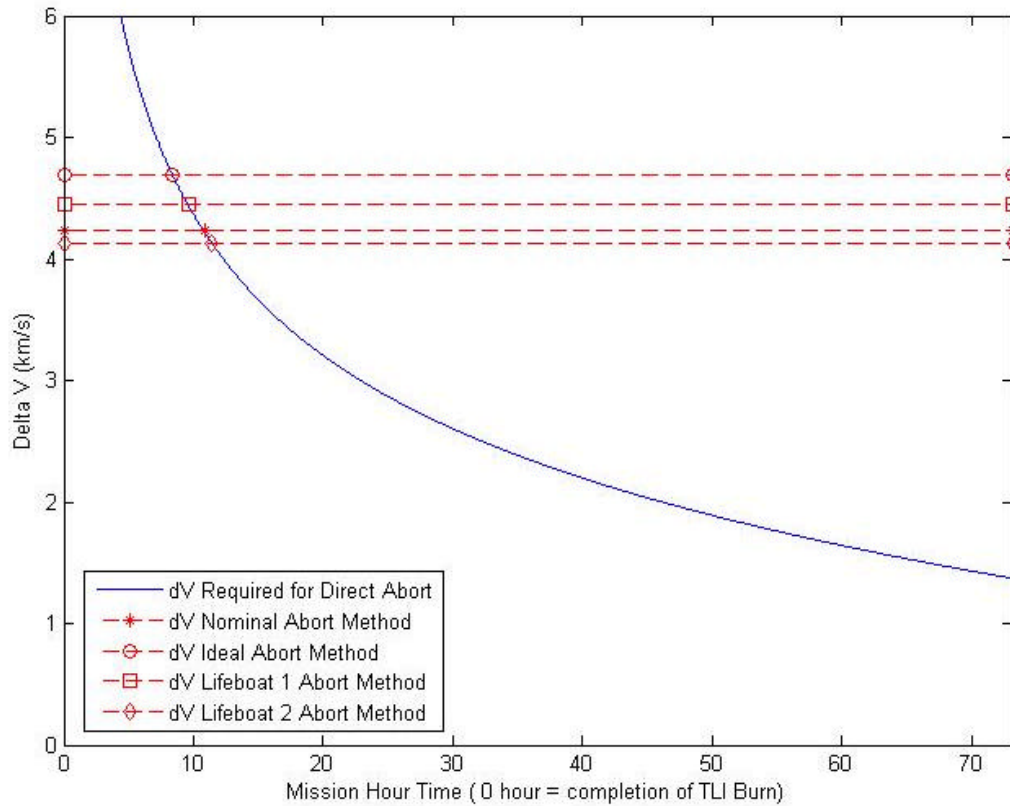
Figure 5.8 Feasibility profiles for various abort methods for the CEV

Figure 5.9 illustrates the abort feasibility regions on a schematic of the trans-lunar trajectory. The feasibility boundaries are positioned to scale for the CEV ideal abort scenario. The various different methods' ΔV capabilities and subsequent Infeasibility region magnitudes are summarized in Table 5.3.

72

Table 5.3 CEV abort methods infeasibility region data

| Method | Effective Delta V (km/s) | Infeasibility Region Data (hrs) | | |
		Duration	1st Boundary	2nd Boundary
Nominal	4.235	10.75	.07	10.82
Ideal	4.697	8.32	.08	8.40
Lifeboat 1	4.443	9.56	.08	9.64
Lifeboat 2	4.132	11.34	.07	11.41
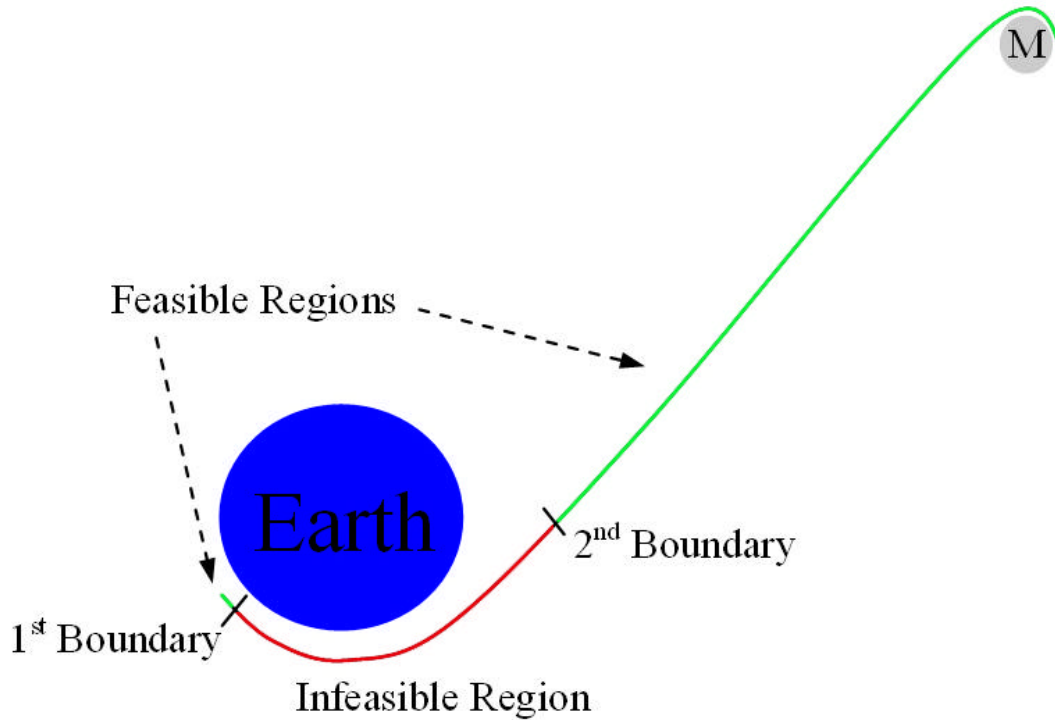
Figure 5.9 Abort feasibility trajectory schematic

As shown in Table 5.3, the duration of abort infeasibility for the ideal abort method in the CEV is 8.32 hours, yet in this time approximately 26% of the radial distance to the moon has been traversed. For the worst case scenario of the nominal abort (the lifeboat case 2 would not be practically considered) the second boundary as shown in Figure 5.9 would be approximately 31% the radial distance to the moon. A potentially significant factor to consider is this is

relatively close to the boundary of the Earths magnetosphere. The resulting implication is that in the event of a solar radiation event leading to an abort scenario, the potential to limit crew exposure to exo-magnetospheric space is very promising. This is a marked improvement to that of the Apollo spacecraft, where the second feasibility boundary for the nominal abort method does not occur until approximately 51% of the radial distance to the moon.

Again referring to Table 5.3; although the ideal abort method for the CEV does not achieve the same improvement over the nominal abort as the Apollo spacecraft, an 11% gain in effective ΔV resulting in a 23% reduction in infeasibility region magnitude is still significant.

Returning to the example presented in the Apollo mission analysis; presuming an emergency situation occurring just after completion of the TLI maneuver would result in a worst case 16.6 hour time to re-entry. The 16.6 hour worst case TOF takes into account coasting until the threshold of abort feasibility as well as the equal flight time for the return trajectory. The overall expansion of the abort feasibility region for the CEV results in a shorter time of flight for direct abort trajectories. In addition to this is an increased excess fuel margin remaining subsequent to the abort maneuver; implying further possibilities for higher energy return trajectory optimization.

5.2.3.   Model Verification

Verification of the model can be ascertained via application of Lambert's Theorem utilizing the universal variable formulation. Lambert's theorem defines a trajectory via two position vectors and a time of flight between them.[16] The theorem states that the time required to transfer between the two radii is dependent only on the semi major axis, the sum of the two radii, and the chord length of the orbital transfer.   The chord lengths and two radii from the problem definition satisfy two of the three quantities required in Lambert's Theorem. The final quantity of semi-major axis is the only unknown parameter and can be stipulated via manipulation of the time of flight equation, such that the time of flight can be written as a function of the semi-major axis. The time of flight equation presented is in Section 3.2, equation (10).   The universal variable formulation of the time of flight equation is shown below.[16]

$$\Delta t = \frac{x^3 S + A\sqrt{y}}{\sqrt{m}} \tag{21}$$

Equation (21) is based on the universal variable x and is also a function of S, A and y defined below.

$$x = \sqrt{\frac{y}{C}} \tag{22}$$

$$S = \frac{\Delta E - \sin \Delta E}{\Delta E^3} \tag{23}$$

$$A = \pm\sqrt{r_0 r(1 + \cos \Delta V)} \tag{24}$$

$$y = r_0 + r + \frac{A(zS - 1)}{\sqrt{C}} \tag{25}$$

Where:

$$C = \frac{1 - \cos\sqrt{z}}{z} \tag{26}$$

$$z = \Delta E^2 \tag{27}$$

The solution to Lambert's theorem follows from iteration of equation (21) via equations (22) through (27) until the desired time of flight for the transfer is attained.

Utilizing the universal variable formulation of the time of flight equation to solve Lamberts theorem allowed a direct validation of the created model. The solution to Lambert's Theorem yielded the velocity of the transfer trajectory at each radii. These velocities could then be compared to the outbound TLI velocity and a ΔV could be calculated. Five sample data points were selected along the outbound TLI trajectory. The ΔV requirement for direct abort was calculated via the developed model and compared with the ΔV requirement found via Lambert's Theorem; results are summarized in Table 5.4.

Table 5.4 Comparison of calculated DV requirements

Mission Hour	Required ΔV for Direct Abort (km/s)		% Difference
	Model	Lambert	
12.3	4.002	4.129	3.2
16.6	3.501	3.600	1.9
23.0	3.001	3.063	2.1
34.2	2.501	2.549	1.9
46.3	2.000	2.042	2.1

Mission hour refers to the time during the TLI trajectory that a direct abort is performed. The sample data set shows a close correlation between the developed astrodynamic model and the solutions via Lambert's Theorem.

Lambert's theorem forms a trajectory based on two position vectors and a time of flight creating a new trajectory rather then reflecting the outbound TLI trajectory as does the model. In addition Lambert's theorem involves no accommodation for assuring a re-entry trajectory. Re-entry trajectories have a tightly constrained range of magnitude and orientation of the velocity vector; application of Lambert's theorem often does not satisfy these constraints. Lambert's method could be modified via addition of an engine burn just prior to re-entry interface to match these constraints; however the ΔV requirement for a maneuver in close proximity to Earth far outweighs its counterpart maneuver far from Earth at the point of direct abort initiation. The lack of re-entry trajectory accommodation in Lambert's method precludes its use as a basis for the model,

however this does not preclude its value in direct abort ΔV requirement verification.

5.2.4. Direct Comparison of CEV and Apollo Abort Capabilities

A primary goal in performing an abort trajectory analysis on both the CEV and Apollo spacecraft utilizing the same mission trajectory is to directly compare the capabilities of each. The common trajectory allows this, but in addition the utilization of the Apollo XV mission trajectory allowed verification with flight data. The model was run with the Apollo mission parameters and confirmed via matching results with flight data.

Perhaps a foreseeable outcome of the CEV design criteria is the increased abort capabilities of the CEV. In order to take a larger crew, as well as achieve global lunar access, increased propulsion capabilities over the Apollo spacecraft are inherently necessary. That combined with the re-distribution of primary mission propulsive responsibilities, such as the lunar module descent stage taking over the LOI burn from the service module as was the case with Apollo, has had a positive impact on abort feasibility. Such a beneficial outcome in fact that the ideal abort method became the optimum choice in terms of effective ΔV which is coincidentally the optimum choice in terms of maintaining life support and consumable resources for the return trip. Figure 5.10 illustrates a summary

of the effective ΔV capabilities for both the Apollo and CEV spacecrafts as presented in Sections 5.2.1 and 5.2.2.
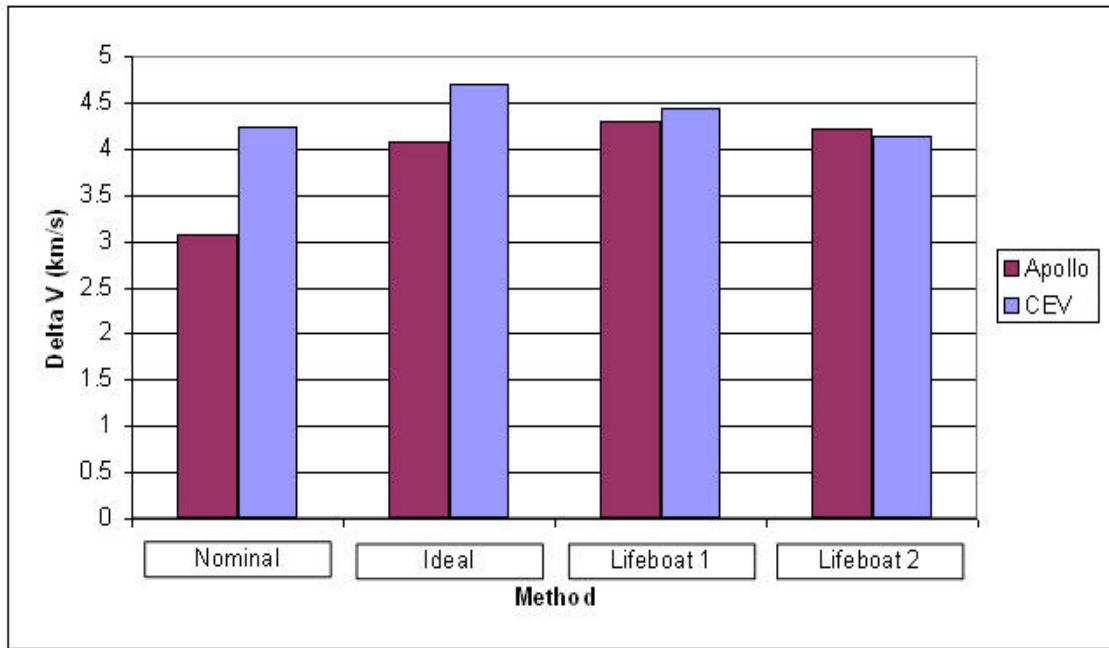
Figure 5.10 Apollo and CEV effective DV capabilities

A comparison of the direct abort infeasibility regions for both spacecraft across the various abort methods is presented in Figure 5.11 Apollo and CEV infeasibility regions. The abort infeasibility region for the mission is inversely related to the abort capabilities of the spacecraft. A reduction of the infeasibility region allows an increase in crew survivability in the event of an emergency situation requiring a direct abort. The reduced infeasibility region not only enables abort trajectories across a larger range of the entire translunar trajectory,

but also enables faster return to re-entry via aborts earlier in the trajectory or a larger excess fuel margin for trajectory optimization.
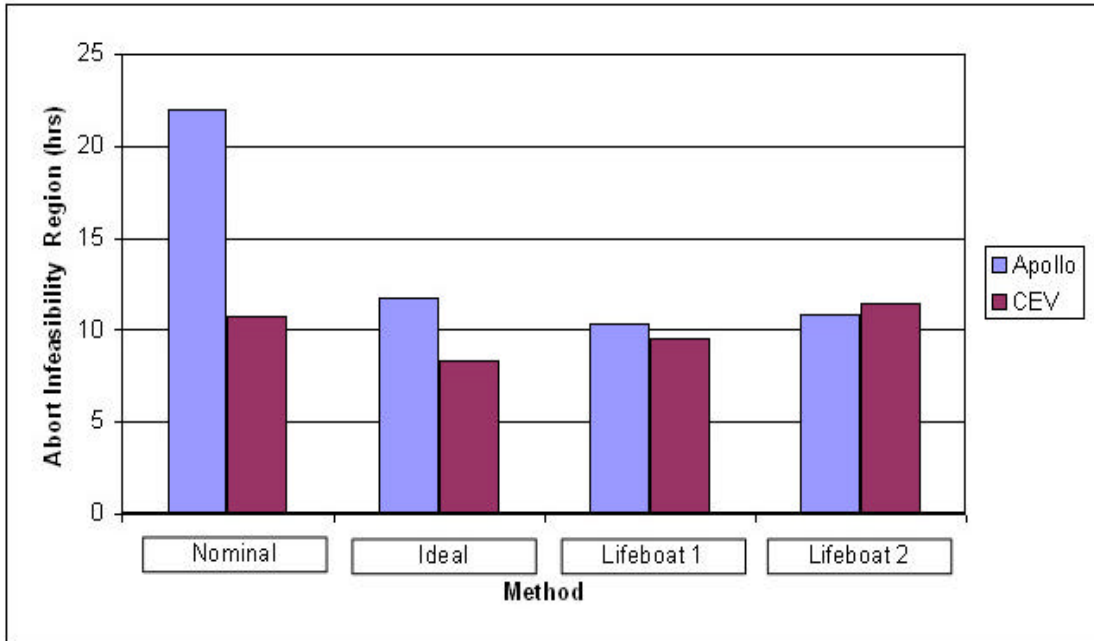
Figure 5.11 Apollo and CEV infeasibility regions

While the previous plots have compared the Apollo and CEV spacecrafts and their corresponding regions of abort infeasibility for the various abort methods, a different perspective is presented in Table 5.5. The Apollo XIV trajectory was the lowest energy translunar injection, while the Apollo XV trajectory was the highest energy translunar injection utilized. Results for each of the spacecraft mass fraction models across the four different abort staging methods are presented. A promising general trend can be seen when comparing

the two spacecraft, overall the CEV has lower infeasibility magnitudes, translating to a generally increased abort capability over the Apollo spacecraft.

Table 5.5 Upper/Lower energy trajectory bounded infeasibility regoins

Mission	Abort Staging Method Infeasibility Region (hours)			
	Nominal	Ideal	Lifeboat 1	Lifeboat 2
Apollo Spacecraft				
XIV	15.93	8.38	8.07	8.06
XV	21.7	11.6	10.26	10.76
CEV Spacecraft				
XIV	9.79	7.67	8.75	10.34
XV	10.69	8.28	9.51	11.34

The only case where the Apollo spacecraft exceeds the abort capabilities of the CEV is on a higher energy trajectory utilizing the lifeboat 2 abort case. The reason for this is simple, due to a departure in design of propulsive responsibilities of each module of the CEV from Apollo the mass ratios do not benefit. In this case the CEV lunar descent module is tasked with performing the lunar orbit insertion burn and thus has a comparatively larger propulsion system. Other than that specific case, which has already been discussed to be less then ideal, the CEV as a whole possesses a marked improvement in abort capability over the Apollo spacecraft. Of particular interest is the ideal abort case in which the abort capabilities of the CEV on the higher energy trajectory exceed that of the Apollo spacecraft on its lower energy trajectory. The two mission trajectory data points for each abort method and each spacecraft serve as a bounding pair. Specifically, the lower energy trajectory for the CEV ideal abort

81

case of 7.67 hours, combined with the higher energy trajectory for the same case of 8.28 hours set the upper and lower bounds for the magnitude of the infeasibility region of that method for the spacecraft. These bounds are however subject to the practicality of the set of Apollo trajectories. Proposed trajectories for the CEV are not currently available, hence the Apollo mission basis, but the abort infeasibility region can easily be substituted upon determination of future CEV mission trajectories.

5.3. Abort Feasibility Across the Range of Possible Translunar Trajectories

An important question is the effect of translunar injection velocity on the magnitude of the abort feasibility envelope. A trade study was performed comparing time of travel to the moon and the period in which direct abort would not be possible. Examination of this trade study was performed via iteration of the astrodynamic trajectory model across the range of possible trajectories characterized by TLI velocity. Included in this investigation was a budgeted fuel margin to also study the effect of reasonable fuel margins on time of abort infeasibility. In other words, if a faster transit time trajectory is chosen, can a certain fuel margin allow for an abort feasibility envelope characteristic of a lower energy trajectory? The goal is to obtain the best of both strategies; fast transit time and abort feasibility across an increased portion of the transit.

With this in mind the length of time of abort infeasibility was used as a figure of merit, as illustrated in Figure 5.12 for the Apollo nominal abort case. As a point of reference, Apollo 15 used 10.8445 km/s TLI velocity. Figure 5.13 shows the same analysis utilizing the percent of total transit time during which an abort is infeasible. The percentage of mission time analysis is presented to gain a better understanding of the extent of the abort feasibility envelope, because as the transit time decreases, the time of abort infeasibility increases, until above a certain TLI velocity an abort will not be possible at any point in the trajectory.
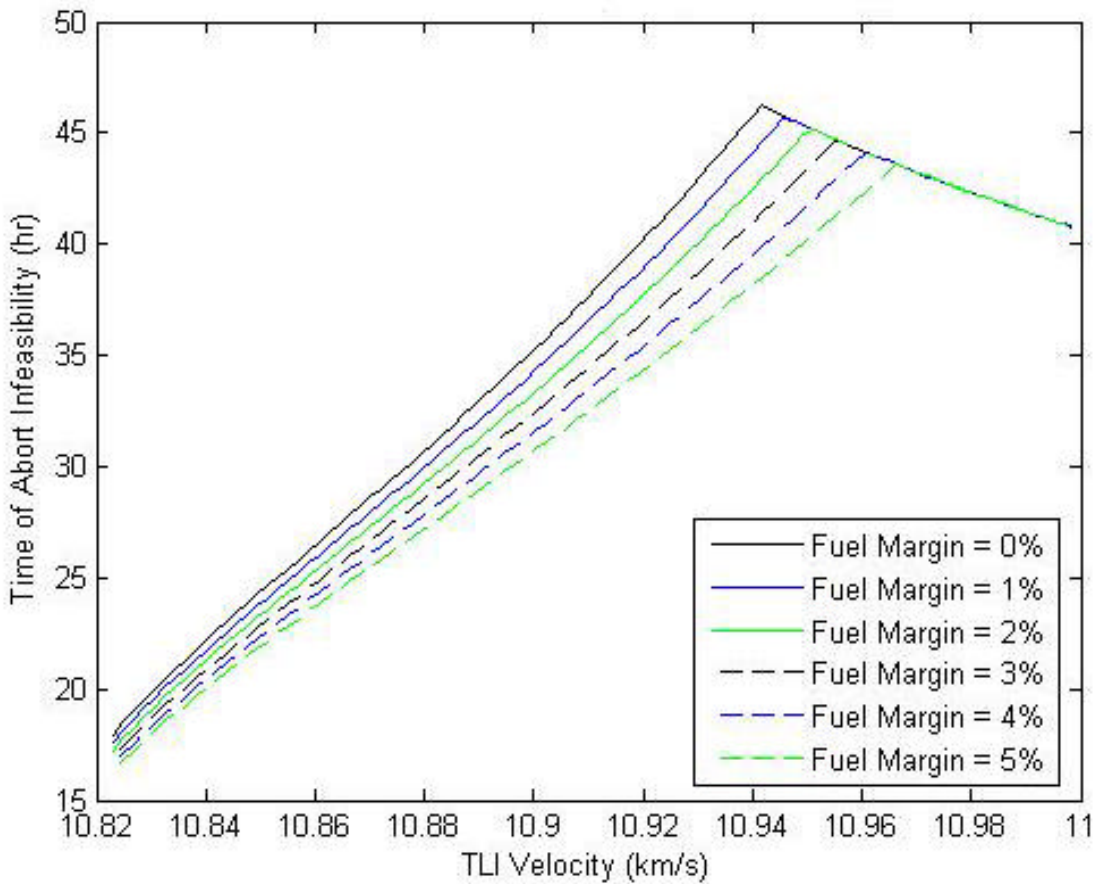
Figure 5.12 Abort infeasibility versus translunar injection velocity
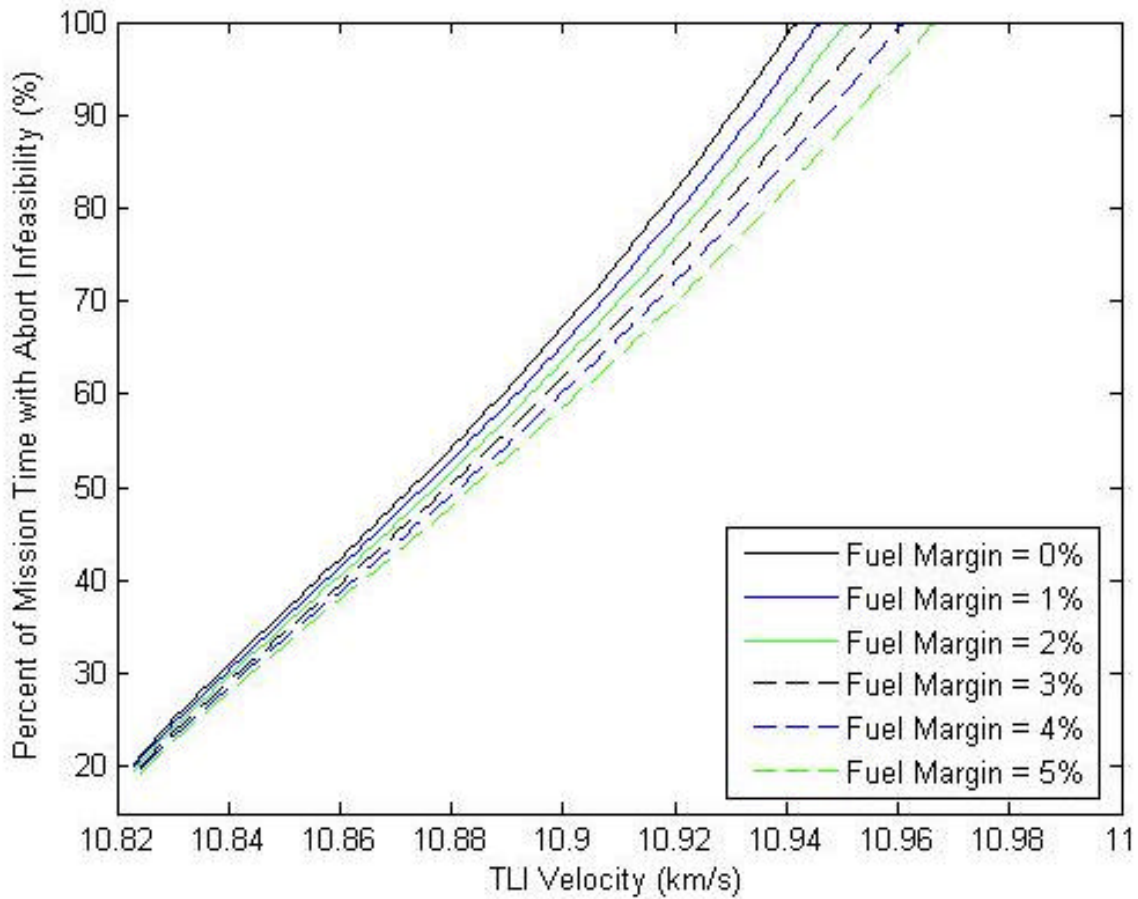
Figure 5.13 Percent of mission abort infeasibility versus translunar injection velocity

The same trade study was conducted for the CEV spacecraft. The ideal abort method was used as it was the most beneficial option for ΔV and life support. Figure 5.14 illustrates the trends for the CEV; due to increased abort capabilities for the CEV the sensitivity to translunar injection velocity is diminished compared to the Apollo spacecraft. A possible benefit could be further flexibility in mission design, allowing for higher energy transfers while still maintaining abort feasibility.
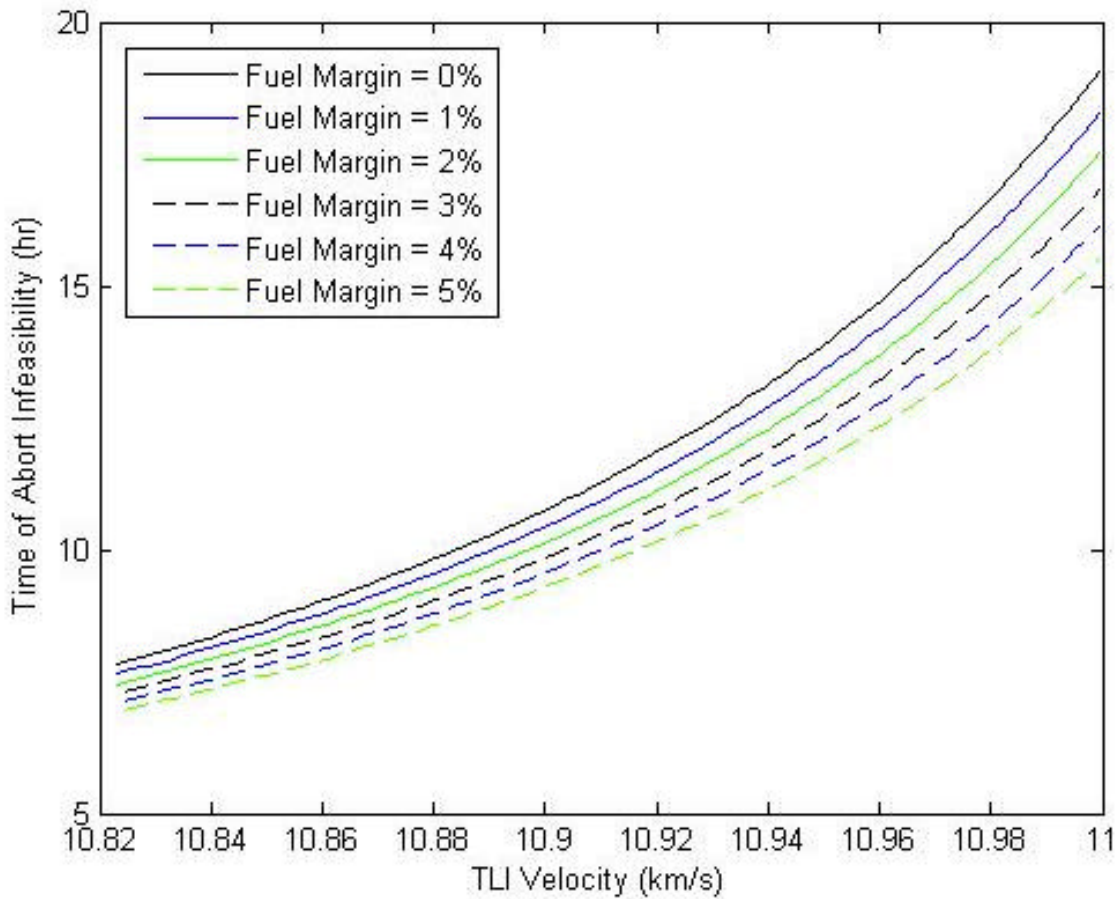
Figure 5.14 Abort infeasibility versus translunar injection velocity for ideal abort in the CEV

In an effort to maintain perspective on the meaning of the slow growth of the abort infeasibility region with TLI velocity the same data is plotted as a function of the infeasible percent of transit time. The trend shown in Figure 5.15 draws out the conclusion that the magnitude of the abort infeasibility region is not necessarily the only concern. In the example of an 11 kilometer per second TLI velocity the infeasibility region is only approximately 18 hours, which is less then the nominal abort case for Apollo, appearing at first glance to be acceptable.

85

However this infeasibility region represents approximately 47% of the total lunar transit time.
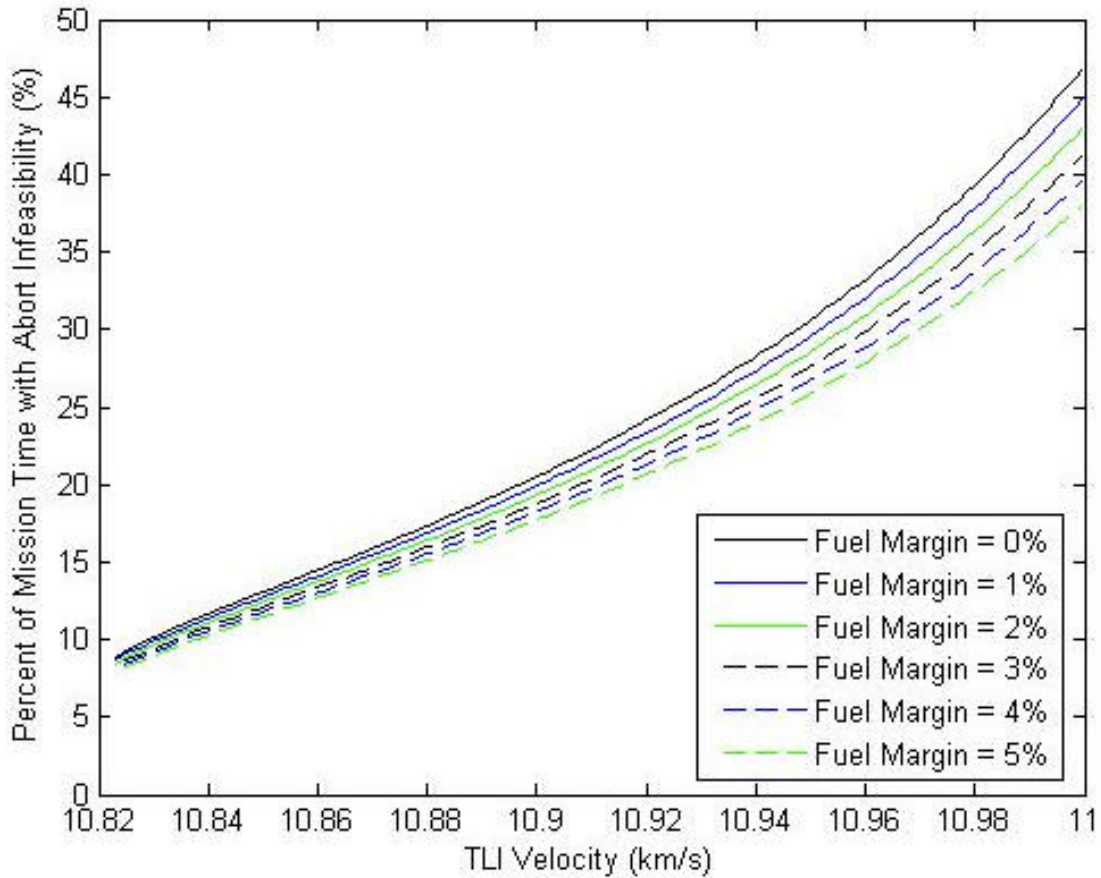
Figure 5.15 Percent of mission abort infeasibility versus TLI velocity for ideal abort in the CEV

Whereas a TLI velocity closer to the Apollo XV reference trajectory has approximately 8.8 hours of direct abort infeasibility, yet this represents less then 12% of the total transit time. An opposing set of trajectory design philosophies is revealed in the trends:

1)   Design for high final TLI velocity (reducing transit time) with the theory that shorter transit time equates to statistically reduced possibility for an emergency abort scenario occurring.

2)   Design for low final TLI velocity (lengthening transit time) with the idea that increasing the abort   feasibility over the mission out weighs the added statistical chances of an emergency abort scenario occurring.

Present results suggest that the first design philosophy would generally have prohibitively high ΔV requirements. ΔV fuel budgets for that end of the spectrum range as high as 2 km/s in excess of Apollo mission parameters. A more beneficial strategy would be to blend the two design philosophies, by designing for a higher TLI velocity to reduce transit time but build in a larger fuel margin to in effect decrease transit time while holding the abort feasibility envelope constant. Further system reliability studies would be required to determine trade offs between shorter transit time combined with reduced abort capabilities, versus longer transit times containing much higher abort feasibility options.

5.4.   *Expedited Return During Feasible Direct Aborts*

The available excess fuel was divided up into two burn portions, one portion to accelerate the transfer orbit to a higher energy trajectory, and one to

decelerate just prior to re-entry to match re-entry corridor conditions. This division of available fuel is shown in Figure 5.16 for the second segment of abort feasibility for the Apollo nominal abort scenario. Mission hour time was utilized as the independent variable for these plots such that if a direct abort is initiated at 'X' hours into the translunar injection, data for that position along the trajectory can easily be found by referencing mission time on the plots. The acceleration burn to attain a higher energy return trajectory is the difference between the solid and dotted line, while the ΔV shown by the dotted line is that required just prior to re-entry to match corridor conditions. Of note on this plot is the difference in the relative magnitude of the acceleration and deceleration burns with respect to the near-Earth mission segment due to the large radial distances from Earth during this portion of the lunar transit. Angular momentum must be conserved, thus a small impulse of ΔV far away from Earth translates to a much larger ΔV required to negate the increased angular momentum in close proximity to Earth, namely, just prior to re-entry to assure compliance with re-entry corridor conditions.
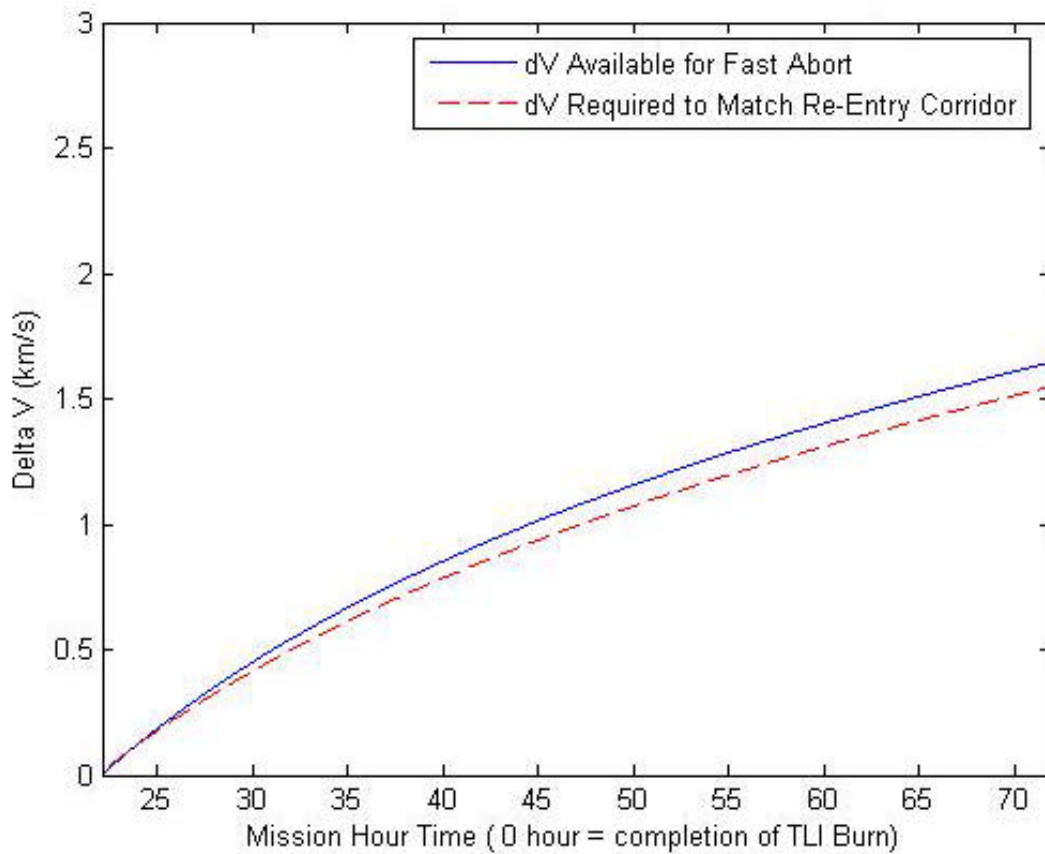
Figure 5.16 Apollo XV division of DV high energy return

A higher energy return trajectory enables a reduction in return to re-entry time for the spacecraft. Also plotted as a function of mission hour, this reduction in flight time can be examined in Figure 5.17, where the dotted line represents the return time to re-entry of a standard abort, and the solid line represents the return time for the optimized higher energy trajectory.
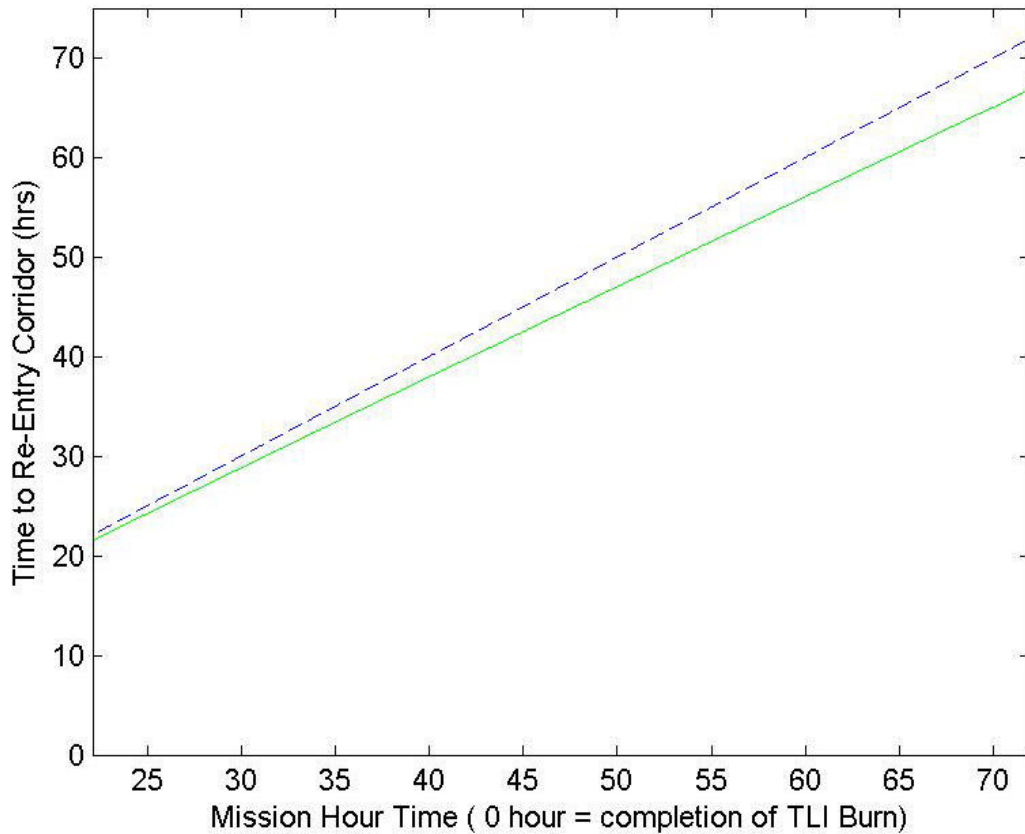
Figure 5.17 Apollo XV nominal abort, higher energy trajectory reduction in return time

The first segment of abort feasibility has been omitted from the optimization as the altitude range is fairly small, and since the CEV transit time through this altitude range is on the order of 3-4 minutes, no optimization of excess fuel was required. An abort during the first segment of abort feasibility during the mission will require fast recognition of the problem and action, and has already been deemed highly improbable. If the near-Earth abort window is missed, approximately 10-15 hours are required until the next region of abort

90

feasibility. Secondly, simply reflecting the orbit via the abort will yield the same flight time to re-entry of 3-4 minutes; which is short enough not to require acceleration (recalling that engine burns are considered to be instantaneous for the model). The instantaneous change of ΔV assumed in the astrodynamic model is fine for flight times on the order of hours; however with a flight time of 4 minutes or less, engine burn time will become a large factor requiring further study. Thus if a direct abort can be executed in such a short time a simple reflected abort is all that is necessary due to extremely short flight times.

Upon examining Figure 5.17 a best case reduction in flight time of approximately five hours is apparent. However this is for the Apollo spacecraft, taking into account the additional abort capabilities of the CEV, further benefits can be realized. Figure 5.18 shows the division of ΔV for an optimized higher energy return trajectory from an ideal abort method in the CEV.
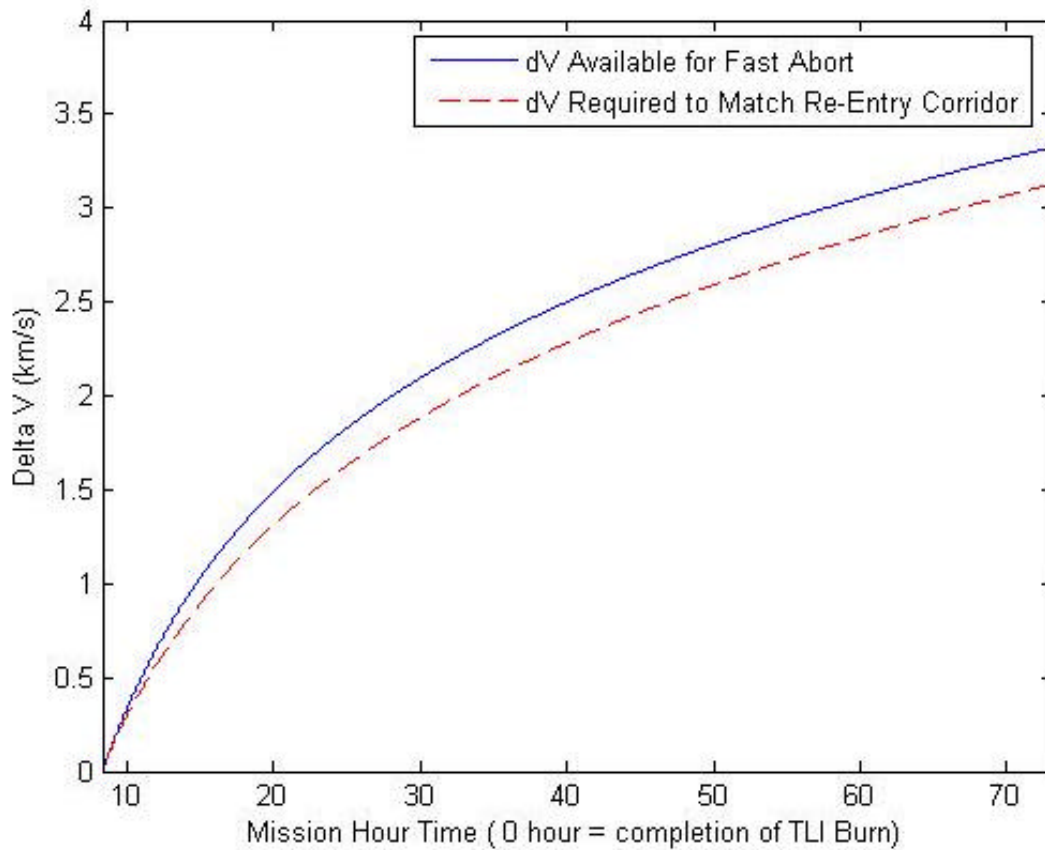
Figure 5.18 CEV division of DV high energy return

Figure 5.19 illustrates the benefit in return time of flight for the optimized higher energy trajectories for the CEV. As before, the dotted line represents the standard direct abort return time, while the solid line represents the achievable return time. Lastly to quantify the gain in return time Figure 5.20 shows a plot of the reduction in flight time via the higher energy transfer orbit.
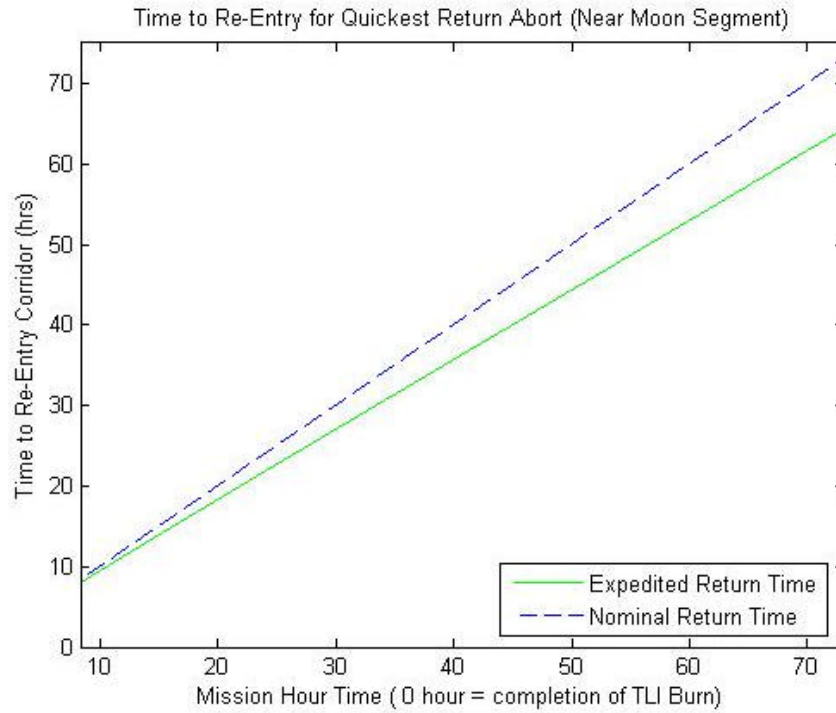
Figure 5.19 CEV ideal abort, higher energy trajectory reduction in return time
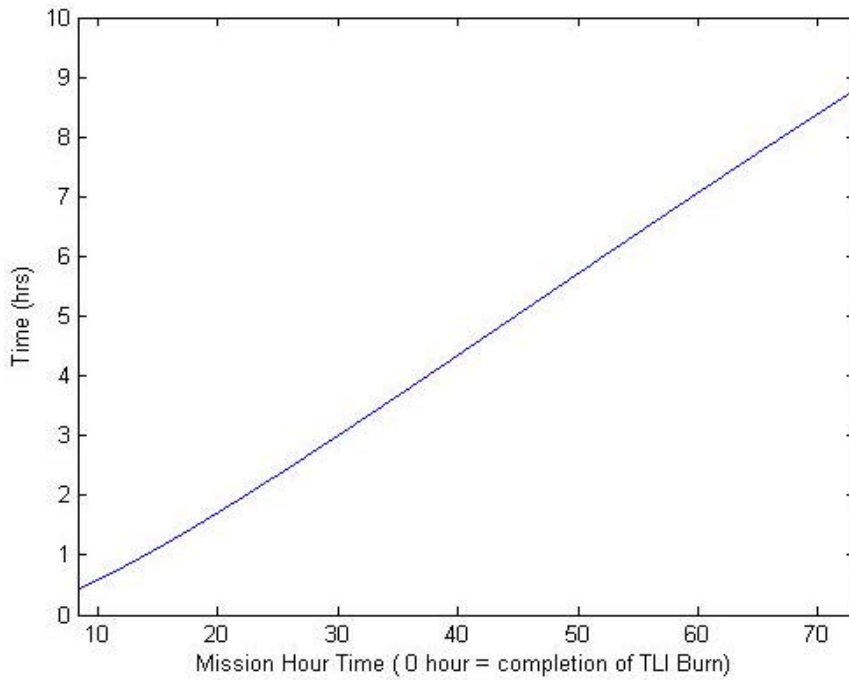
Figure 5.20 Reduction in return time for ideal CEV abort as a function of mission time of abort initiation

A factor of 12% reduction in return time could potentially be vital depending on emergency situational concerns, fading life support, environmental conditions, etc. Most importantly this higher energy return trajectory is simply using fuel that would otherwise remain in the tanks un-utilized, wasted. In practicality the direct abort ΔV maneuver and the ΔV maneuver to initiate the higher energy transfer could be combined into a single engine burn.

5.5. Return During Infeasible Region, Pseudo-Direct Aborts

The very nature of the problem holds grim outlook for this analysis in terms of finding a panacea trajectory to return to Earth. The model was created with a Sequential Quadratic Programming (SQP) method of minimization in an attempt to search the abort trajectory design space for any unforeseen feasible options. It has already been established that even for an ideal abort method the CEV does not have the effective ΔV capability to perform a direct abort in this region to the translunar trajectory. The optimization sought to discover any feasible trajectories utilizing two or more segments, in effect, pseudo-direct aborts.

The objective function for the optimization scheme was that of time of flight for return. This was chosen because if minimizing ΔV was utilized, many

trajectories would have been expected, however all with much too long time of flight characteristics. A well known tradeoff in astrodynamics is that between time of flight and ΔV required for the maneuver, the lower the ΔV for the maneuver, the longer the time of flight to reach the destination. For the case of finding a return trajectory for the CEV, the shortest time of flight was desirable. Namely due to the length of the infeasibility region; at approximately eight hours long any feasible trajectory would need a time of flight for return to be less then 16 hours. This is assuming a worst case scenario where a direct abort is required just after completion of the TLI burn. If the pseudo-direct abort has a longer time of flight than simply waiting until the threshold of direct abort feasibility and returning on a direct abort, than it is not a reasonable choice.

Inherent to the optimization is significant computational time due to many iterations of the objective function. In the case of this model, the objective function was required to be solved twice for each design iteration, once for the actual objective function, and once again as a component of the nonlinear constraint. In consequence, specific data points were chosen along the trajectory to analyze.

Nearly 70 data points were evaluated in close proximity to the feasibility threshold due to the lower required ΔV for a direct abort in these regions. Although prohibitively high for a direct abort, the required ΔV for a direct abort was low enough to be considered potentially achievable via pseudo-direct abort

methods. Figure 5.21 illustrates some of the data points, represented by vertical lines, based on mission time of a theoretical emergency requiring an attempted pseudo-direct abort.
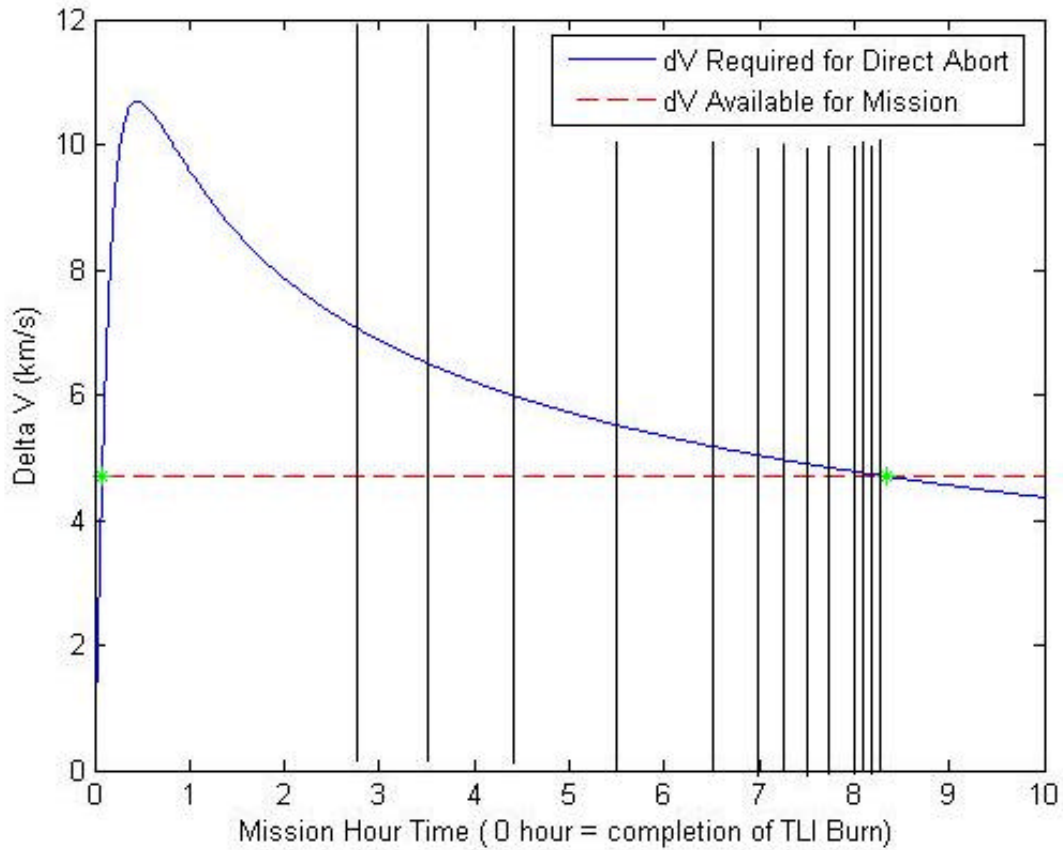

Figure 5.21 CEV ideal abort, example data point locations

Each of 23 specific mission hour times was evaluated at potentially three different trajectory options, two, three, or four intermediate burns. Not every trial run resulted in a closed trajectory sequence. As the pseudo-direct abort method is built one trajectory segment at a time, it was possible and quite likely

for the trajectory not to close. Meaning the optimizer could not find either a local or global minimum. In this case, since the SQP method is gradient based, it is reasonable to assume it should converge on any possible solution fairly quickly, and a maximum of 1000 was set on the function evaluations.

Out of 23 data points including three different burn combinations at each point, 14 trajectories did close. Of those 14, six of the trajectories required far too much ΔV. The model was set up such that if the ΔV constraint was violated but a closed trajectory sequence was found it would report the required ΔV. Of other eight trajectories returned, six violated the ΔV constraint, leaving two viable trajectories. However of the six violating the ΔV constraint, the maximum was only 1.5 kilometers per second, higher, or approximately 30%. Table 5.6 gives the data of the best five trajectories found and their associated performance gains

Table 5.6 Pseudo-direct abort trajectories

# of Burns	Abort Time	% Over dV budget	% Return Time Savings
3	7.15	-2.59	27.27
2	8.205	5.49	13.91
2	7.39	13.12	35.99
3	3.51	14.92	27.07
3	2.84	21.45	28.87

A major point of note is the first trajectory is in fact a feasible closed pseudo-direct abort trajectory. In addition it also affords a 27% savings in return time. The second trajectory is also worthy of note, specifically due to its ability to save almost 14% in return time via an approximately 5% fuel increase.

These results, while not a very high success rate regarding the number of data points vs. number of useful trajectories, do hint at a small niche of trajectory design space. That although a single burn direct abort is not feasible, it is possible to slightly 'gray' the feasibility boundaries utilizing intermediary trajectories to form a pseudo direct abort sequence.

When viewing the raw trajectory data and interesting point emerges. The algorithm utilized worked backwards form the re-entry corridor through the pseudo-direct abort sequence to the original abort initiation position. In this matter there is a trajectory matching burn that is calculated from the reverse sequence such to match the entire sequence to the original outbound TLI prior to abort, in effect closing the trajectory and defining a solution. Examining the ΔV burn data and the optimizer selected coast times for the intermediate trajectories reveals that the viable pseudo-direct abort trajectories closely mimic the form of the direct abort trajectory. They all have a single major abort initiating burn, followed by a long coast. However, subsequent trajectory segments are for the most part very short coasting times, on the order of minutes, and tend toward radii closer to Earth implying that the feasible pseudo-direct aborts in general form verify that the direct abort method is in fact a correct strategy. By allowing the optimizer to determine coast times and ΔV maneuvers, it is able to select the best method for an abort, and when its selected method mimic the original conceived direct abort, it verifies the concept. However few the actual closed

pseudo-direct abort trajectories were, they did serve to verify the direct abort method. The pseudo-direct abort model was created to allow for any number of intermediary burns in the trajectory sequence. A range of two to four was chosen based on reliability and risk of firing main propulsion systems numerous times in an emergency situation. It was presumed that the least number of ΔV maneuvers required was preferred. To that effect the design variable vectors were set up as a function of desired number of burns, flexible to any number. Thus, verification of both models against each other was possible. By picking a data point in the feasible region and setting the number of intermediary burns to one, the model created for the infeasible region requiring a pseudo-direct abort, should in effect mimic the direct abort model. Upon inputting a feasible data point at mission hour 8.99, a direct abort trajectory was returned with a time of flight of 8.58 hours. Which at first glance is within 4.7% of the direct abort model results; however, referring to Figure 5.20, for a abort initiated at approximately nine hours mission time, utilizing all available fuel a drop of approximately 0.4 hours is expected in return time. Taking this approximately 0.4 hours into account with the 8.58, results in approximately 8.98 hours compared to 8.99 hours. Briefly, the pseudo-direct abort study provided a check for any missed trajectory methods that were not thought of, verified the direct abort concept, and allowed verification of data for both models.

Chapter 6.　　Conclusions and Implications

Following the comprehensive trajectory analysis presented in Chapter 5; Chapter 6 details flexibility of the developed model to handle future lunar missions. In addition, conclusions specific to the CEV are presented along with a quick overview of possible future work.

6.1.　Flexibility of Abort Trajectory Study

With regards to future applications the work completed thus far has been aimed at creating a resource to be utilized for mission planning and potentially spacecraft capability for any future lunar missions.

Flexibility between the Apollo spacecraft example and the CEV, as well as any other lunar bound spacecraft for that matter, can be easily adapted into the model via mass ratios and ΔV performance data. The spacecraft mass data is included in the calculation of the mission budgeted ΔV for the spacecraft based on trajectory profile. It is then converted from the budgeted ΔV to an effective ΔV for each type of abort method based on staging mass fractions. The four abort methods are defined via mass fractions; simply rearranging the mass fractions can create new abort staging methods.

Upon complete evaluation of the four abort methods it is the ideal abort method which clearly is the primary choice for an abort during a CEV lunar mission. This method not only provides the maximum effective ΔV, thereby increasing feasibility of a direct abort, it also retains the largest possible habitable volume, and presumably available consumable resources contained on the LSAM ascent stage, for the duration of the return trajectory.

Another point of note concerning various abort staging methods and their application to optimized higher energy return trajectories is that of biased ΔV for the deceleration burn. The vast majority of ΔV expenditure is just prior to re-entry due to conservation of angular momentum. In close proximity to Earth it takes a large amount of ΔV to affect a small change in angular momentum. The consequences of this directly impact the available habitable volume and life support resources for the crew during a higher energy return trajectory. Since the accelerating burn requires such little ΔV it is likely that the first module jettisoned may not be jettisoned until the remainder of its fuel is depleted at the beginning of the decelerating maneuver. Therefore by virtue of a large bias in ΔV towards matching re-entry corridor conditions, further life support capabilities than expected from examination of abort staging methods, may exist for the duration of the return.

In addition to flexibility on spacecraft ΔV determination via mass ratios and abort methods, the model has been designed with a reasonably wide range

of trajectories. Theoretically an infinite number of possible trajectories is available by varying the translunar injection altitude and velocity. Noting; however, that velocity should be kept below 11.2 kilometers per second for manned missions regardless due to reaching near-Earth-space escape velocity and attaining hyperbolic trajectories. Given the flexibility in spacecraft capability characterization as well as trajectory definition, this work should be adaptable to any future manned lunar mission.

6.2. Practicality & Conclusions for the CEV

Originally constructed around Apollo mission data as a basis, the model has since been updated with all available CEV mass estimations and propulsion system forecasted capabilities. Rationale for a necessitating a direct abort has been explained. Emergency situations can arise from mechanical, environmental, or other concerns such as health. If such a situation does arise, several staging options have been examined and their effective ΔV capabilities analyzed. The intent of the study was to characterize the feasibility of a direct abort situation for the CEV. As such the first objective was an easy inspection based method by which to ascertain abort feasibility via profile plots like that of Figure 5.3 which characterize both the ΔV requirements and capabilities of the spacecraft for various abort staging methods. Next, a SQP optimization scheme was utilized to best distribute excess fuel margin after a direct abort maneuver in

order to attain the fastest return to Earth possible while still within the constraints of the re-entry corridor. Following optimized higher energy trajectory return optimization, a trade study was conducted to examine the effects of varying TLI velocity as well as fuel margin. It was deemed possible to affect a higher energy TLI trajectory with the same feasibility region as a lower energy transfer if sufficient fuel margin was budgeted. For a spacecraft such as the CEV being designed for global lunar access, it is likely to be utilized on missions that are not reaching its propulsion capabilities limits. During such missions, the ability to decrease transit time may be possible while maintaining constant abort feasibility profiles via fuel margin.

Another possible concept to consider when designing the CEV is the sensitivity of fuel margins to specific spacecraft modules on the overall abort feasibility. To this effect a fuel margin of 5 and 10% was applied to each propulsion module of the CEV stack; Table 6.1 summarizes the results of this analysis for the CEV utilizing the ideal abort method.

Table 6.1 Specific module fuel margin sensitivity on abort infeasibility

Module	% Fuel Margin	Total ΔV Available (km/s)	% Total ΔV Increase	Infeasibility Duration (hrs)	Reduction of Infeasibility Duration (hrs)	% Reduction Infeasibility Duration
Service	5	4.769	1.5	7.959	.361	3.8
	10	4.842	3.1	7.658	.662	7.4
LSAM AS	5	4.726	.6	8.144	.176	1.6
	10	4.756	1.3	8.016	.305	3.1
LSAM DS	5	4.829	2.8	7.708	.612	6.8
	10	4.962	5.7	7.188	1.132	13.1

For point of reference the infeasibility duration for the CEV on an ideal abort is 8.32 hours. The service module as well as the LSAM ascent stage both achieve a relatively marginal gain in abort feasibility via increased fuel margin. However the mass ratio advantage combined with added propulsive responsibility for the LSAM descent stage grants a distinct advantage to abort feasibility via increasing the LSAM descent stage fuel margin. The relative mass of the LSAM DS compared to the other module, and its added responsibility of performing the LOI burn to circularize the CEV stack in LLO demands a larger fuel capacity. Inherently the LSAM DS is the most desirable module to lend a fuel margin; resulting in a 6.8% and 13.1% increase in abort feasibility from 5 and 10% fuel margins respectively. The design recommendation of maximizing the fuel margin for the LSAM DS holds a two fold advantage. Primarily the direct influence of added fuel margin to increasing abort feasibility; but the recommendation also inherently improves the possibility of further lunar access via landing site flexibility.

Converse to the fuel margin advantages is the situation of a spacecraft mass over budget on design mass. The need to reduce mass of the spacecraft could be represented by a negative fuel margin. In that respect the same fuel margin study is expanded into the negative percentage range to represent the impact on abort feasibility of reducing fuel by a given negative margin. Table 6.2 below parallels Table 6.1; a key focus is the negative reduction in infeasibility

region. This negative reduction increases the duration of the abort feasibility

region.

Table 6.2 Specific module negative margin sensitivity on abort infeasibility

Module	% Fuel Margin	Total ΔV Available (km/s)	% Total ΔV Increase	Infeasibility Duration (hrs)	Reduction of Infeasibility Duration (hrs)	% Reduction Infeasibility Duration
Service	-10	4.550	-3.1	8.955	-.679	-8.2
	-5	4.624	-1.5	8.607	-.332	-4.0
LSAM AS	-10	4.637	-1.3	8.546	-.270	-3.3
	-5	4.667	-.6	8.490	-.215	-2.6
LSAM DS	-10	4.431	-5.7	9.571	-1.295	-15.6
	-5	4.564	-2.8	8.894	-.619	-7.5

Figure 6.1 illustrates the linear behavior of the sensitivity of the abort infeasibility

profiles with respect to fuel margin. The impact of small fuel margins (+ or −

10%) for specific modules on the total available ΔV for an abort can be estimated

from this plot.
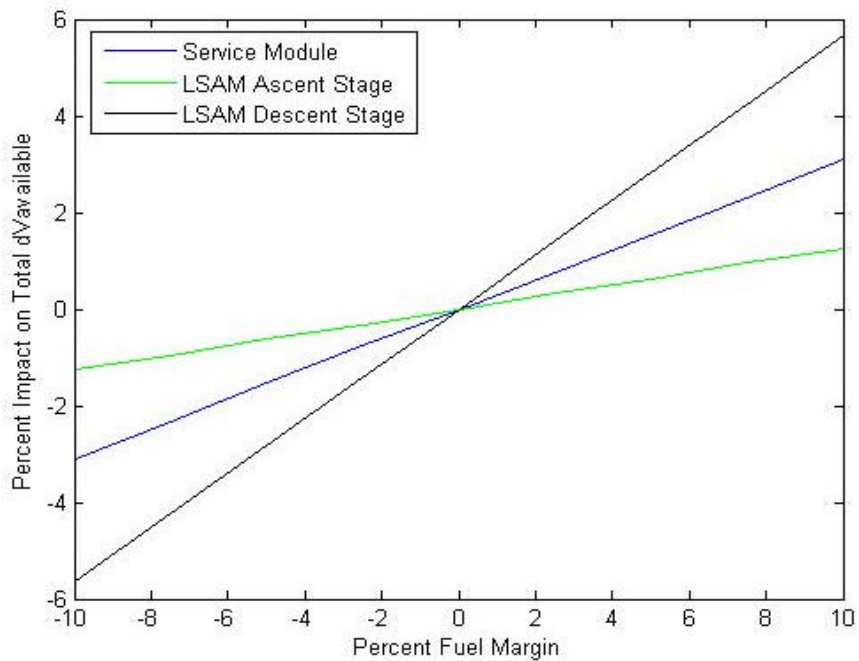
Figure 6.1 Impact of fuel margin on available DV

From another point of view the impact of fuel margin on ΔV available for abort can be examined based on mass. During the design of the CEV if a specified amount of mass can be allotted to fuel margin, then Figure 6.2 shows the percent fuel margin for a specific module that is achieved by adding a specified amount of mass to the fuel budget. The percent fuel margin attained from Figure 6.2 can then be examined via Figure 6.1 to yield the final impact on ΔV available for abort from a specified added fuel mass.
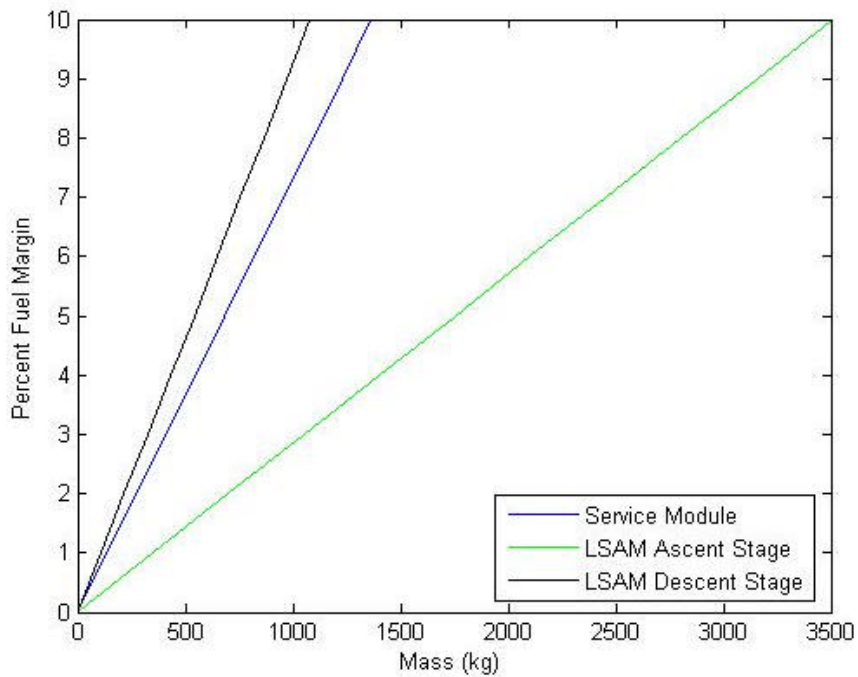

Figure 6.2 Percent fuel margin from added fuel mass on a specific module

In the situation of spacecraft module mass being larger than the budgeted design mass Figure 6.2 can be applied to affect a negative fuel margin as well. For a

106

specified value of kilograms over budget, the percent fuel margin required to

reduce the fuel mass to within overall budgeted mass can be found. Figure 6.1

can than be used to determine the level of increased abort infeasibility from

decreasing the fuel load on a specific module. From the trends in these two plots

two design strategies drop out. The first for the case of positive design margin,

where there exists space in the mass budget to allow addition of fuel. In this case

the optimum choice, from the perspective of maximizing abort feasibility would

be to increase the fuel capacity of the LSAM Descent stage. As is shown in

Figure 6.1, this module yields the greatest benefit to total ΔV available for the

addition of fuel. The second case of a negative design margin where the

spacecraft mass is currently greater then the budgeted design mass, a reduction

in mass must be made. For this case it is clear from Figure 6.2 the ideal module

to reduce the fuel mass of, again from the standpoint of maximizing abort

capabilities, is the LSAM Ascent Stage. This module would allow the lowest

percent fuel margin for a given specified reduction in kilograms of fuel. When

applied to Figure 6.1 as a negative fuel margin, it yields the lowest impact on

total ΔV available. Thus utilizing the studied fuel margin of specific modules can

offer a significant benefit to designing for abort capability during the CEV design

phase.

A further recommendation directly impacting the abort feasibility of the

CEV is that of flexibility of attitude control. Given the technological advances in

computing power since the days of Apollo it is not unreasonable to recommend

an inter-module controllability. Given that an emergency situation requiring a

direct abort could include unforeseen circumstances, the ability to control any

given propulsion system from any module would be a distinct advantage for

crew survivability. It would almost negate entirely the need for a manually

targeted direct abort via centering the Earth in the docking reticle. For example

an inter-module propulsion control system could allow the LSAM DS propulsion

system to be controlled by the service module Guidance, Navigation, and

Control (GNC) computer. Or any other combination thereof; the situation of a

manually targeted course correction arose on the Apollo XIII mission due to

limited power constraints prohibiting the use of the GNC computer. The ability

to control the propulsion system of one module from the pilot seat of another

module would not only eliminate this problem and increase abort feasibility, but

also increase reliability via GNC redundancy. In conjunction with recommended

inter-module propulsion controllability would be a recommendation for the

design of robust RCS capabilities. The redundancy of RCS capability between

modules would increase odds of guaranteed abort feasibility. The loss of RCS

ability for any given module should not negate the ability to utilize the primary

propulsion system of the module. If an inter-module GNC capability exists it

follows that the RCS of one module should be designed robust enough such that

control of the entire spacecraft stack can be achieved while a second module is

providing primary prolusion.   The Apollo spacecraft nearly achieved this capability; the only exception was the LM AS RCS system was not robust enough to control the spacecraft while docked with the CSM.   Given the mass ratio changes in the CEV design constituting the decrease in relative size of the SM compared to the LSAM AS, it would seem reasonable to impose the recommendation of a more robust RCS system.   Overall the design recommendations of inter-module GNC compatibility as well as completely robust RCS design for any possible spacecraft module stack combination will positively impact the ability and available abort options during an emergency situation.

Lastly, of major accomplishment was the establishment of a pseudo-direct abort method, opening up the possibility for the fast return of a spacecraft to Earth via intermediary trajectories.   The use of the SQP optimizer allowed generic trajectory definition, in an effort to look for other trajectory methods not previously considered.   Given the CEV's improved abort feasibility over that of the Apollo spacecraft; the possibility exists to potentially perform a pseudo-direct abort entirely within the Earth's magnetosphere.   This method of abort would definitely be recommended in the case of abort due to solar radiation concern and consequently bears value in future mission design studies.

As a side benefit from the need to create this second optimizer as a completely autonomous model, it enabled the verification of trajectory

information from the original model. This combined with comparison of trajectory profiles to both Apollo flight data and Lambert's method trajectory solutions, yields a high confidence in the model.

6.3. Future Work

There are two limitations to the models created in this study. First they are both based in 2-D, assuming all maneuvers occur in the plane of departure for the translunar trajectory. Plane changes are accounted for in a "worst case" plane change factor method, however a fully 3D model could provide further accuracy for abort feasibility characterization. Secondly, the primary motivation in this study has been to bring the crew of the spacecraft home as quickly and safely as possible. In line with this reasoning it was deemed more desirable to land anywhere on the earth than remain in space during an emergency situation. To this effect, landing foot print magnitude or location has been neglected. While its inclusion would require a specific launch date, the inclusion of landing site tracking in the trajectory analysis could add options for mission control. If for instance a direct abort was required, but there exists enough time to loiter in orbit and land in a predetermined location this may be a desirable function to be included in the model.

Further work may cover trajectory analysis through re-entry taking into account aero-thermodynamic effects. Or perhaps examine off design trajectory re-entry. Fully understanding the extents of limitations on flight path angle and re-entry velocity could be useful in abort situations. Allowing a higher re-entry velocity could enable a faster return by utilizing less fuel to slow the spacecraft at the re-entry interface.

This study has characterized the feasibility and requirements for various abort trajectories as well as offered optimization of these trajectories. The newfound understanding can offer the crew of any future manned lunar mission the best possible chances for a safe return in the event of an abort scenario.

Bibliography

[1] "Exploration Systems Architecture Study: Final Report (ESAS)." NASA, November 2005. NASA-TM-2005-214062. www.sti.nasa.gov

[2] "Crew Exploration Vehicle," NASA RFP NNT05AA01J, Attachment J-1, http://prod.nais.nasa.gov/cgi-bin/eps/sol.cgi?acqid=113638

[3] Lozier, David. Galal, Ken. "Lunar Prospector Mission Design and Trajectory Support." AAS 1998-323

[4] Hoekstra, T.B. "The Abort Capabilities of the Apollo Spacecraft on the Translunar Trajectory." Bellcomm, Inc., TM-68-2013-3. June 25th 1968.

[5] Anselmo, D.R. Baker, M.K. "Translunar and Lunar Orbit Abort Trajectories for Apollo 14." Bellcomm, Inc., B70-12019, December 7th 1970.

[6] Stern, R. J. "Preliminary Evaluation of SM/RCS Capability to Abort to Earth Entry from the Relaxed Free Return Profile." Bellcomm, Inc., B70-09084, September 30th 1970.

[7] Bass, R. A. "Optimization of Hybrid Trajectories for the Apollo Mission Under a DPS Abort Constraint." Bellcomm, Inc., B69-02018, Febraury 7th 1970.

[8] Babb, Jr., Gus R. "Translunar Abort Techniques for Non-Free-Return Missions." NASA, TM X-1806

[9] Foggatt, Charles E. "Manual Abort Maneuvers During the Translunar Coast Phase of a Lunar Mission." NASA MSC Internal Note 66-FM-140, November 21st 1966.

[10] Vaughan, W. W., Niehuss, K. O., Alexander, M.B. "Spacecraft Environments Interactions: Solar Activity and Effects on Spacecraft" NASA Reference Publication 1396, November 1996

[11] "New Vision for Space Exploration Program Announcement." President George W. Bush, January 14th 2004. http://www.whitehouse.gov/news/releases/2004/01/20040114-3.html

[12] Larson, Wiley J., Pranke, Linda K. *Human Spaceflight: Mission Analysis and Design.* McGraw-Hill, New York.

[13] Apollo by the Numbers: A statistical Reference," NASA Historical Reference, SP-4029, Table: Launch Vehicle/Spacecraft Key Facts. http://history.nasa.gov/SP-4029/Apollo_18-12_Launch_Vehicle-Spacecraft_Key_Facts.htm

[14] "Apollo LM" http://www.astronautix.com/craft/apollolm.htm September 19th 2005.

[15] "Apollo CSM" http://www.astronautix.com/craft/apollocsm.htm September 19th 2005.

[16] Bate, Roger R., Mueller, Donald D., and White, Jerry E. *Fundamentals of Astrodynamics*, Dover Publications, New York, 1971.

[17] Vinti, John P., *Orbital and Celestial Mechanics*, Volume 177 in Progress in Astronautics and Aeronautics, AIAA, Reston, 1998.

[18] Escobal, Pedro R., *Methods of Orbit Determination*, Volume John Wiley & Sons, New York, 1965.

[19] Vallado, David A. *Fundamentals of Astrodynamics and Applications, Second Edition.* Microcosm Press/Kluwer Academic Publishers, El Segundo, 2001.

[20] Beksinski, E. David; Starkey, R. P.; Lewis, M.J. "Characterization of Feasibility, Methods, and Requirements for Lunar Mission Abort Trajectories" AIAA/AAS Space Flight Mechanics Conference, Tampa, January 22nd 2006. AAS-114

[21] Puetrobon, Steven S., "Lunar Orbit Propellant Transfer," Small World Communications, 1999.

[22] "Preliminary Apollo Abort Study Trajectory Analysis." Space Technology Laboratories, Inc., N79-76209, November 12th 1963.

[23] "Apollo by the Numbers: A statistical Reference," NASA Historical Reference, SP-4029, Table: Translunar Injection. http://history.nasa.gov/SP-4029/Apollo_18-24_Translunar_Injection.htm